JOINT TRANSPORTATION
RESEARCH PROGRAM
INDIANA DEPARTMENT OF TRANSPORTATION
AND PURDUE UNIVERSITY

Use of LRFR Methodology for Load Rating of INDOT Steel Bridges

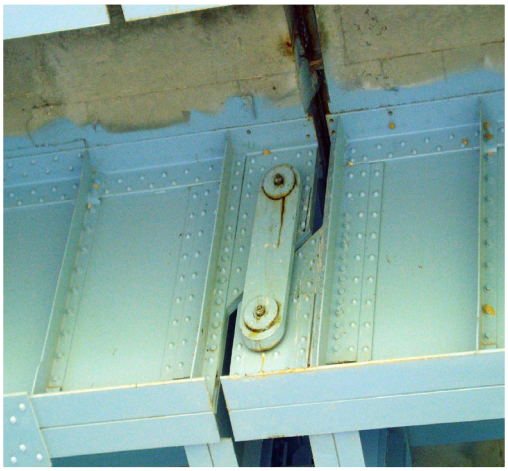

Prekshi Khanna, Mark D. Bowman

SPR-4229 • Report Number: FHWA/IN/JTRP-2021/37 • DOI: 10.5703/1288284317362

RECOMMENDED CITATION

Khanna, P., & Bowman, M. D. (2021). *Use of LRFR methodology for load rating of INDOT steel bridges* (Joint Transportation Research Program Publication No. FHWA/IN/JTRP-2021/37). West Lafayette, IN: Purdue University. https://doi.org/10.5703/1288284317362

AUTHORS

Prekshi Khanna
Graduate Research Assistant
Lyles School of Civil Engineering
Purdue University

Mark D. Bowman, PhD, PE
Professor of Civil Engineering
Lyles School of Civil Engineering
Purdue University
(765) 494-2220
bowmanmd@purdue.edu
Corresponding Author

JOINT TRANSPORTATION RESEARCH PROGRAM

The Joint Transportation Research Program serves as a vehicle for INDOT collaboration with higher education institutions and industry in Indiana to facilitate innovation that results in continuous improvement in the planning, design, construction, operation, management and economic efficiency of the Indiana transportation infrastructure. https://engineering.purdue.edu/JTRP/index_html

Published reports of the Joint Transportation Research Program are available at http://docs.lib.purdue.edu/jtrp/.

NOTICE

TECHNICAL REPORT DOCUMENTATION PAGE

1. Report No. FHWA/IN/JTRP-2021/37	**2. Government Accession No.**	**3. Recipient's Catalog No.**
4. Title and Subtitle Use of LRFR Methodology for Load Rating of INDOT Steel Bridges		**5. Report Date** November 2021
		6. Performing Organization Code
7. Author(s) Prekshi Khanna and Mark D. Bowman		**8. Performing Organization Report No.** FHWA/IN/JTRP-2021/37
9. Performing Organization Name and Address Joint Transportation Research Program Hall for Discovery and Learning Research (DLR), Suite 204 207 S. Martin Jischke Drive West Lafayette, IN 47907		**10. Work Unit No.**
		11. Contract or Grant No. SPR-4429
12. Sponsoring Agency Name and Address Indiana Department of Transportation State Office Building 100 North Senate Avenue Indianapolis, IN 46204		**13. Type of Report and Period Covered** Final Report
		14. Sponsoring Agency Code

15. Supplementary Notes

Conducted in cooperation with the U.S. Department of Transportation, Federal Highway Administration.

16. Abstract

Load rating of bridges before 1994 was primarily conducted by Load Factor Rating (LFR). In 1994, the American Association of State Highway and Transportation Officials (AASHTO) developed and encouraged the use of a probabilistic-based method titled Load and Resistance Factor Design (LRFD) for carrying out bridge design. A new methodology consistent with LRFD was also developed and adopted for conducting load rating. Thus, a new Load and Resistance Factor Rating (LRFR) was adopted by AASHTO in 2001 for load rating. Today, the bridges that were designed by the old LFD methodology are rated by both LFR and LRFR. Continued development suggests that load rating in future will be based only on LRFR, therefore LRFR is the recommended method for carrying out load rating of bridges even if they were designed by LFD. The Indiana Department of Transportation (INDOT) encountered some LFD designed bridges which were adequate by LFR methodology (i.e., produced a rating factor of more than 1.0) but inadequate for LRFR. The load ratings were carried out using AASHTOWare Bridge Rating (BrR) software. These bridges belonged to five different limit states: (1) lateral torsional buckling, (2) changes in cross-section along the member length, (3) tight stringer spacings, (4) girder end shear and (5) moment over continuous piers. This research study explores the inherent differences between LFR and LRFR to clarify some of the inconsistencies in the rating values. Load ratings for select bridges were carried out using both AASHTOWare BrR and a separate analysis using Mathcad and structural analysis results from SAP2000 for comparison purposes. Finally, the study also recommends some modifications in the BrR software input data that can be adopted for each of the above-mentioned limit states to resolve inconsistencies found between LFR and LRFR rating values.

17. Key Words load rating, LRFR, AASHTOWare BrR, lateral torsional buckling, moment gradient, tight stringer spacings, LL distribution factor	**18. Distribution Statement** No restrictions. This document is available through the National Technical Information Service, Springfield, VA 22161.

19. Security Classif. (of this report) Unclassified	**20. Security Classif. (of this page)** Unclassified	**21. No. of Pages** 51	**22. Price**

EXECUTIVE SUMMARY

Introduction

A method for examining the load carrying capacity of a structure is Bridge Load Rating. It is a process of determining the structural condition and safety of a bridge. Load rating typically utilizes bridge information obtained from the plans, design calculations, or field information to conduct a structural analysis and evaluation to determine if the bridge is safe for public use.

The current preferred methodology used for load rating is Load and Resistance Factor Rating (LRFR). Before LRFR, load rating was carried out by using either Load Factor Rating (LFR) or Allowable Stress Rating (ASR) methods. The American Association of State Highway and Transportation Officials (AASHTO) developed a powerful software called AASHTOW are Bridge Rating (BrR). The software is compliant with the *LRFD Bridge Design Specifications*. Today, many of the State Departments of Transportation (DOTs) use this software to carry out comprehensive load ratings of structures.

The Indiana Department of Transportation (INDOT) expressed a desire to use just one load rating method (LRFR). Although the shift from LFR to LRFR over the years has ensured more consistent decisions regarding the safety of bridges, there are some shortcomings. It was observed that LFR and LRFR methodologies produced different rating factors for the same structure. INDOT has reported that in some bridges AASHTOWare BrR indicated a bridge was satisfactory for LFR ($RF > 1$) but not adequate for LRFR ($RF < 1$). These bridges belonged to a few different limit states: lateral torsional buckling, changes in the cross section along the member length, tight stringer spacing, girder end shear, and moment over continuous piers.

Findings

The limit states discussed earlier were examined for select bridges that generally satisfied LFR rating but were inadequate for LRFR evaluation. LRFR was found to be appropriate for most applications. However, for a few limited situations, recommendations were suggested for adapting the AASHTOWare BrR for LRFR with modification to the input information.

For the limit state of lateral torsional buckling, the calculation of the moment gradient modifier, C_b for all non-prismatic sections, is assumed to be equal to 1.0, which is a conservative approach. To rectify this, a new method to calculate C_b is suggested for stepped beams (or non-prismatic sections).

Another recommendation concerned the modelling of tapered, partial length cover plates in AASHTOWare BrR. AASHTOWare BrR uses a conservative approach to calculate the effective width of tapered cover plates. Instead, a new approach based on the principles of direct proportion of the width within the length in which it occurs is used.

For tight stringer spacings, it was observed that the controlling factor for the resulting lower rating factor values by LRFR was the calculation of the live load distribution factors. The formulae in the *LRFD Bridge Design Specifications* (AASHTO, 2020) that calculate LL distributions can be used only if the girder characteristics fall in the range of applicability. If the characteristics are not applicable, then the lever rule is used to calculate the LL distributions—this approach is based on statics and often produces higher than anticipated LL distribution factors (LLDF). This approach results in higher live load effects and lower rating factors. To improve the results produced by lever rule, use of a technique called Henry's method is suggested to calculate moment LLDF for stringers with tight spacings (less than 3.5 ft.).

The final limit state addressed was girder end shears and moment over continuous piers. For this limit state, the 14 bridges that were examined earlier for lateral torsional buckling, along with two additional bridges, were reviewed. It was observed that apart from two bridges, all the other bridges were adequate for shear. These two bridges showed an abnormal spike in the shear values within the length of the girder; therefore, it is believed that the modeling and analysis of the girders in AASHTOWare BrR was flawed. The bridges that were inspected earlier for lateral torsional buckling for flexure pass for this limit state as well if the recommendations presented earlier are adopted.

It was observed that the AASHTOWare BrR software generally works well and, other than the possible changes noted in this study, the BrR results should be used. The recommendations suggested in this study can be adopted by INDOT to resolve the problem of inadequacy of bridges by LRFR methodology.

Implementation

AASHTOWare BrR was used extensively to examine the input information for problematic cases. The results from AASHTOWare BrR were compared with the results of detailed Mathcad and SAP2000 analysis. It was concluded that the analysis and capacity calculations conducted by AASHTOWare BrR are according to the provisions of the *LRFD Bridge Design Specifications*. It was observed that there are modifications that can be incorporated into the BrR software input data to provide more accurate results for problematic limit states of bridges designed by LFD. These modifications involve three specific situations.

1. The capacity in BrR can be modified using the "Capacity Override" feature to input the value obtained from using a new C_b for non-prismatic sections.
2. Tapered cover plates can be modelled as a rectangular cover plate by using a new proposed equation for the effective width. The revised width can be manually entered in the BrR software. BrR uses this new cover plate geometry to calculate a new LTB capacity, and thus a new rating factor is generated.
3. For tight stringer spacings less than 3.5 feet, the live load distribution factor computed by Henry's method can be used in BrR by the user inserting the new value. This new value is then used by BrR to compute new moment live load effects, and hence a new rating factor.

CONTENTS

LIST OF TABLES

LIST OF FIGURES

1. PROBLEM DEFINITION

1.1 Introduction and Problem Statement

Highway bridges are an integral part of a nation's infrastructure as they not only make transportation easy and convenient but also bolster the economic growth of the nation. They are one of the most important structural components of a transportation system. It is therefore essential to ensure the safety and maintenance of highway bridges. This is done by carrying out periodic inspections. While visual inspection is critically important, bridges must also be checked periodically for their load carrying capacity and evaluated to determine maximum allowable truck loads on the structure.

A method of examining the load carrying capacity of the structure is Bridge Load Rating. It is a process of determining the structural condition and safety of a bridge. Load rating is done by using bridge information obtained from the plans, design calculations or field information to conduct a structural analysis and evaluation to determine if the bridge is safe for public use.

The current preferred methodology used for load rating is Load and Resistance Factor Rating (LRFR). It is a relatively new methodology which was adopted in 2001 and is consistent with the *LRFD Bridge Design Specifications* (AASHTO, 2020). Before LRFR, load rating was carried out by using either Load Factor Rating (LFR) or Allowable Stress Rating (ASR) methods consistent with the provisions of the *Standard Specifications for Highway Bridges* (AASHTO, 2002).

Bridge Load Rating can be a tedious process as it involves advanced structural analysis of a complex structure with multiple girders. To aid in this process, the American Association of State Highway and Transportation Officials (AASHTO) developed a powerful software called AASHTOWare Bridge Rating (BrR), known as Virtis previously. Today, most of the State Departments of Transportation (DOTs) use this software to carry out comprehensive load ratings of structures.

In the last several years the load rating policy in Indiana was to use LRFR if the bridge was designed by Load and Resistance Factor Design (LRFD) and LFR if the bridge was designed by Load Factor Design (LFD) or Allowable Stress Design (ASD). However, there was a desire by the Indiana Department of Transportation (INDOT) to move to the use of just one load rating method (LRFR). Although the shift from LFR to LRFR over the years has ensured a more consistent decision making regarding the safety of bridges, there are some shortcomings. It was observed that LFR and LRFR methodologies produced different rating factors for the same structure. Due to the inherent differences between the methodologies (as discussed in later sections), the difference in the values of rating factors is evident, but the problem arises when AASHTOWare BrR indicates that a bridge is satisfactory for LFR ($RF > 1$) but not adequate for LRFR ($RF < 1$). INDOT has reported some bridges having this discrepancy in a few different limit states or particular conditions: lateral torsional buckling, changes in the cross section along the member length, tight stringer spacing, girder end shear and moment over continuous piers.

In such a situation it becomes necessary to understand the causes of such differences and their resolution. Decisions regarding either changing the posting limit or modifying the structure to improve the strength would need to be taken if a bridge is not satisfactory for LRFR but passes for LFR.

1.2 Research Objective

As the bridges that were reported by INDOT were adequate for LFR methodology but not for LRFR, the objective of this research was to notice the differences between these two methodologies and understanding the reasons behind those differences. AASHTOWare BrR was used extensively to examine the input information for problematic cases. The purpose was to delve into the details of the calculations conducted by AASHTOWare BrR to suggest possible corrections in the software, if appropriate. A separate girder analysis was also conducted on SAP2000 to find moments and shears for carrying out comparisons with BrR results to assist in understanding the inconsistencies in the rating values.

2. LITERATURE REVIEW

2.1 Load Rating

According to AASHTO's (2018) *Manual of Bridge Evaluation* (MBE), bridge load rating is defined as "The determination of the live-load carrying capacity of an existing bridge." Bridge load rating, thus, provides a basis for determining the safe load capacity of a bridge. Engineering judgement is required to conduct load rating, and to determine a rating value which ensures the safety of the bridge and arrive at posting and permit decisions (AASHTO, 2018). Load rating procedures and criteria for load posting of existing bridges are provided in the MBE (AASHTO, 2018). These procedures are intended for use in evaluating the types of highway bridges commonly in use in the United States that are exposed mainly to permanent loads and vehicular loads. MBE (AASHTO, 2018), however, does not include methods for evaluation of existing bridges for extreme events such as earthquakes, vessel collision, wind, flood, ice, or fire. Rating bridges with long spans, movable bridges and other complex bridges involve additional considerations and loadings which are not mentioned in the MBE (AASHTO, 2018). The load rating of a bridge is based on existing structural conditions, material properties, loads, and traffic conditions. Changes in these parameters could require re-evaluation (AASHTO, 2018). The MBE (AASHTO, 2018) provides the procedures for the Allowable Stress Rating (ASR), Load Factor Rating (LFR), and the Load and Resistance Factor Rating (LRFR) methods.

It states that any of the above methods can be used to establish live load capacities and load limits for purposes of load posting, and no preference is given to any one of the rating methods. INDOT prefers the use of LFR and LRFR over ASR; therefore, these two methodologies are discussed in more detail in the next section.

2.2 Different Methodologies–Load Rating

2.2.1 Allowable Stress Rating and Load Factor Rating

In allowable or working stress method, all the actual loadings together produce a maximum stress in a member which should not exceed the allowable or working stress. The allowable stress is determined by multiplying a factor of safety with the limiting stress of the material. This method of rating can be useful for comparison with past practices. (Armendariz & Bowman, 2018).

The Load Factor method of rating involves analysis of a structure which is subjected to factored loads (which are multiples of the actual loads) (AASHTO, 2018). Load factors consider the uncertainty in the load calculations and there are different load factors for each type of load. The member has adequate capacity when the effect of the factored loads does not exceed the strength of the member. The LFR methodology comprises of two levels or ratings: inventory and operating levels. They are discussed in detail in later sections.

In the Allowable Stress and Load Factor methods, the HS-20 truck or lane loading as mentioned in the *Standard Specifications for Highway Bridges* (AASHTO, 2002) are used for determining the live load force effect.

The general expression for determining the load rating of the structure is given as,

$$RF = \frac{C - A_1 D}{A_2 L(1+I)} \qquad \text{(Equation 2.1)}$$

Where C is the capacity of the member, D is the dead load effect on the member, L is the live load effect on the member, I is the impact factor to be used with live load effect, A_1 is the factor for dead load, and A_2 is the factor for live load.

The values of the constants A_1 and A_2 are different for the Allowable Stress and Load Factor methods. For Allowable Stress method, $A_1 = 1.0$ and $A_2 = 1.0$ in the rating equation, while for the Load Factor method, $A_1 = 1.3$ and A_2 varies from 2.17 for inventory to 1.3 for operating.

2.2.2 Load and Resistance Factor Rating (LRFR)

The Load and Resistance Factor Rating method is consistent with the Load and Resistance Factor Design philosophy (LRFD). Load and Resistance Factor Rating comprises of three different procedures: (1) design load rating, (2) legal load rating, and (3) permit load rating. Each procedure serves a specific purpose and also determines whether there is a need for further evaluations to ensure bridge safety and serviceability (AASHTO, 2018).

The design load rating is a preliminary assessment of bridges based on the HL-93 (discussed in further sections) loading and LRFD design standards. This load rating measures the performance of existing bridges to current LRFD bridge design standards. Under this check, bridges are screened for the strength limit state at the LRFD design level of reliability (inventory) and a second lower level of reliability (operating). Design load rating is like a screening process to identify bridges that should be rated for legal loads. If a bridge passes the design load check ($RF \geq 1$) at the inventory level, it will have sufficient capacity for all the legal loads within LRFD exclusion limits. Bridges that give satisfactory rating factor for design load rating at the operating level are sufficient for AASHTO legal loads but may or may not be adequate for all state legal loads, as some of these loads might be larger than the AASHTO legal loads (Armendariz & Bowman, 2018).

Legal load rating is a second level rating which determines a single safe load capacity (for a given truck configuration) appropriate for both AASHTO and state legal loads. The primary limit state for legal load rating is the strength limit state. Sometimes service limit states are also checked (AASHTO, 2018). Bridges that are not adequate by design load rating are rated for legal loads and thus the outcomes of legal load rating are used to make decisions regarding load posting and bridge strengthening. The vehicular loads used in legal load rating are AASHTO legal loads applied separately or state legal loads.

Permit load rating ensures the safety and serviceability of bridges for vehicles above the weight limits accepted legally. It is a third level rating that is only applied to those bridges which have adequate capacity for AASHTO legal loads. The MBE also mentions the calibrated load factors for checking the load effects of the overweight vehicles (AASHTO, 2018).

Loads that may be significant while load rating are combinations of permanent loads and vehicular live loads. Environmental loads like wind, ice, temperature, stream flow, and earthquake are usually not considered while bridge load rating (AASHTO, 2018).

The general expression for determining the load rating of each component and connection subjected to single force effect (i.e., axial force, flexure, or shear) is given as,

$$RF = \frac{C - (\gamma_{DC})(DC) - (\gamma_{DW})(DW) \pm (\gamma_P)(P)}{(\gamma_{LL})(LL - IM)} \qquad \text{(Equation 2.2)}$$

Where C is the capacity of the component, DC is the dead load effect on the component, DW is the wearing surface effect on the component, P is the permanent loads other than dead loads, LL is the live load effect on the component, IM is the dynamic load allowance

due to the live load, γ_{DC} is the LRFD load factor for dead loads, γ_{DW} is the LRFD load factor for wearing surfaces, γ_P is the LRFD load factor for permanent loads other than dead loads, and γ_{LL} is the evaluation live load factor.

The primary limit state for load rating is the strength limit state; however, the service and fatigue limit states are typically also checked.

2.3 Major Differences Between LFR and LRFR Load Rating

To justify the differences and lower rating factors for LRFR methodology, some fundamental differences between both the methodologies are observed. Murdock (2009) in his research found that the moment and shear rating factors generated by the LRFR methodology are fundamentally lower than the LFR rating factors due to differences in live load distribution factor, live load factors, dynamic load allowance (impact) factors and the capacity of the member. These differences, and some more, are explained in the sections that follow.

2.3.1 Different Design Live Loading

Live loading or vehicles mainly consist of three types: design, legal, and permit. Load Factor Rating (LFR) and Load and Resistance Factor Rating (LRFR) have a significantly different set of vehicles and loadings for design loading. The difference in the models of vehicles leads to a difference in the live load effects such as reactions, moments, and shears produced due to the live load. The following paragraphs discuss these differences in depth.

The design loading for LFR methodology consists of standard trucks or lane loads. For standard trucks, there are four classes: H 15-44, H 20-44, HS 20-44, and HS 15-44. The "44" in the names of these vehicles denotes the 1944 edition when the policy to affix the year to the loadings for their identification was initiated. The H loadings mentioned above comprises of a two-axle truck or corresponding lane load. The number after the letter H denotes the gross weight (tons) of the vehicle (AASHTO, 2002). A standard H truck is shown in Figure 2.1.

HS loadings are larger than the corresponding H loadings. This type of loading includes a tractor truck with semi-trailer or the corresponding lane load. The vehicles are designated by the letters HS and a number indicating the gross weight in tons (AASHTO, 2002). Figure 2.2 shows a standard HS truck.

Lane loading consists of a uniform load combined with a single concentrated load (or two concentrated loads for continuous spans). For H 20-44 and HS 20-44 loadings, the magnitude of uniform loading is 0.64 kip/ft, and the concentrated loads depend on whether bending stresses or shearing stresses are being computed. A lighter concentrated load of 18 kips is used for moment, whereas a heavier load of 26 kips is used for

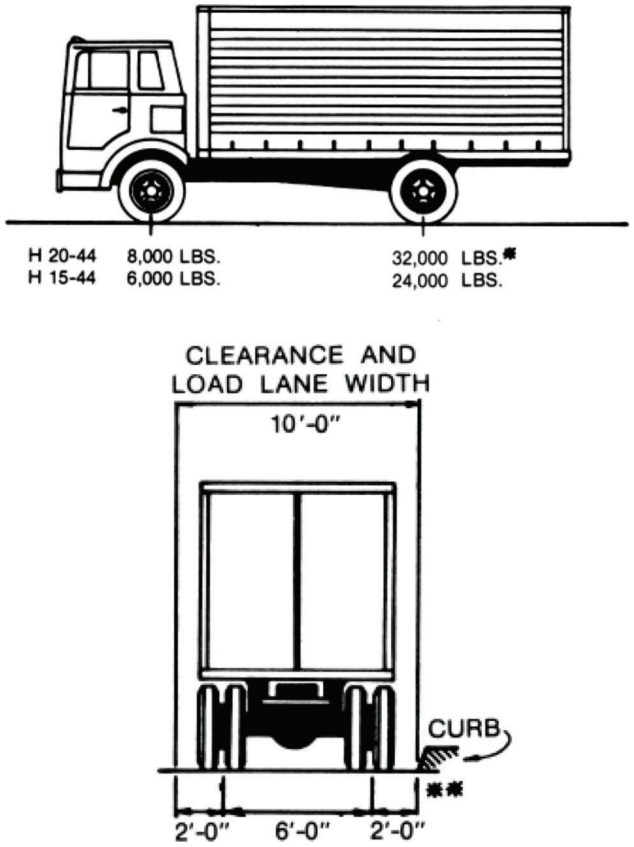

Figure 2.1 Standard H truck configuration (AASHTO, 2002).

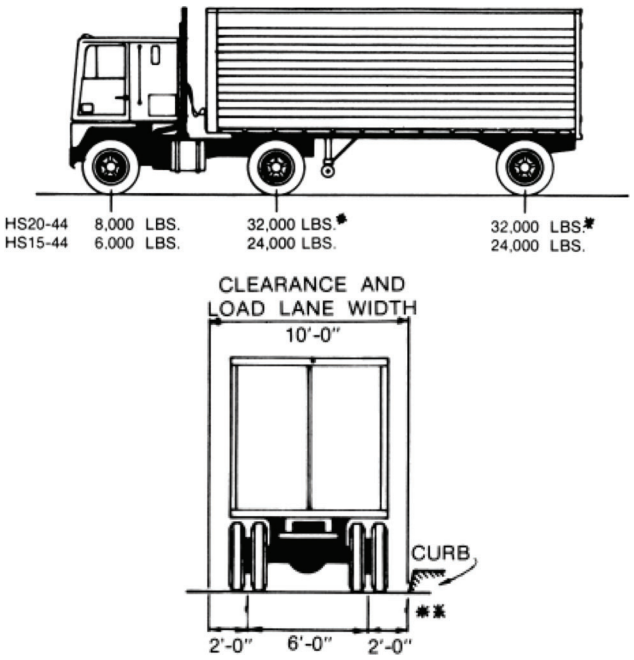

Figure 2.2 Standard HS truck configuration (AASHTO, 2002).

shear. The magnitudes of the concentrated loads are different for H 15-44 and HS 15-44 loadings: 13.5 kips is used for moment and 19.5 kips for shear. Also, a uniform load of 0.48 kip/ft. is used (AASHTO, 2002). Figure 2.3a and 2.3b illustrate the lane loading for H 20 and HS 20, and H 15 and HS 15 loadings, respectively.

In LRFR, the design loading is designated as HL-93 loading and it includes the combined effects of a design truck or design tandem and a lane load. The HL in the name stands for "highway load" whereas 93 represents the year 1993 which signifies the year of its development. The design truck in HL-93 loading is the same as HS 20 Truck and the design tandem consists of two 25-kip axles spaced 4 ft. apart. The design truck or the design tandem (whichever produces a greater force effect) combined with a lane loading of 0.64 kip/ft, is known as the HL-93 live loading (AASHTO, 2020).

For lane loading, HL-93 loading comprises of a 0.64 kip/ft. uniform loading in the longitudinal direction. Unlike the LFR lane loading, there are no concentrated loads for moments and shears in LRFR design loading since it is combined with a truck or tandem load. The LRFR design truck configuration is shown in Figure 2.4.

An essential difference between the design loadings used in the two methodologies is that in LFR, either the standard truck or lane loading is used to compute the force effects, whichever produces larger live load effect. In LRFR, both the truck (or tandem) and lane loading are used together to calculate the live load moments and shears. Thus, it is evident that the design load used in the LRFR methodology is essentially larger than the one used in LFR. The increased loading in LRFR is thereby expected to produce larger effects due to live load, since it is in the denominator part of the rating factor equation, thus leading to a decrease in the rating factor.

2.3.2 Different Live Load Distribution Factors

Live load distribution factor determines the portion of the total live load that a structural member of the bridge resists. LFR and LRFR use different approaches to calculate live load distribution factors. The LFR methodology uses a simplified "S over approach" in which S stands for the lateral girder spacing (AASHTO, 2002). The *LRFD Bridge Design Specifications* (AASHTO, 2020) stipulate the calculation of the live load distribution factors in the LRFR methodology. The LRFR expressions are based on finite element analysis (FEA) and are more intricate when compared to the ones calculated by the LFR methodology. As the calculation is based on FE analysis, the distribution factor calculated by LRFR accounts for factors such as the deck thickness, girder spacing, span length and a longitudinal stiffness parameter. The shift from the straightforward calculation by LFR to a more complex calculation by LRFR is made to achieve more precise values of live load distributions (Lichtenstein Consulting Engineers, Inc., 2001). Detailed expressions for live load distributions under both LFR and LRFR methodologies are explained in Section 4.1. Moen and Fernandez (2009) in their research discovered that the LRFR rating factor for an interior composite steel girder is about 40% lower than the LFR rating factor at operating level of rating; this difference was attributed to the difference in the calculation of live load distribution factors. In another research, the difference between LFR and LRFR rating factors was determined for exterior girders. It was found that LFR ratings were 17.04%–57.50% higher than the LRFR values at inventory level. At operating level, the difference increased to 50.86%–96.66%. This was due to difference in live load distribution factors in LFR and LRFR. (Zheng et al., 2007).

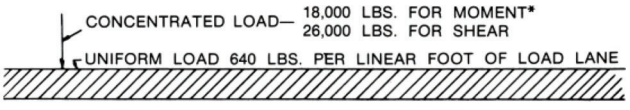

(a) Lane loading for H20-44 and HS20-44 loading

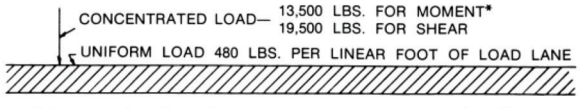

(b) Lane loading for H15-44 and HS15-44 loading

Figure 2.3 Lane loading–LFR (AASHTO, 2002).

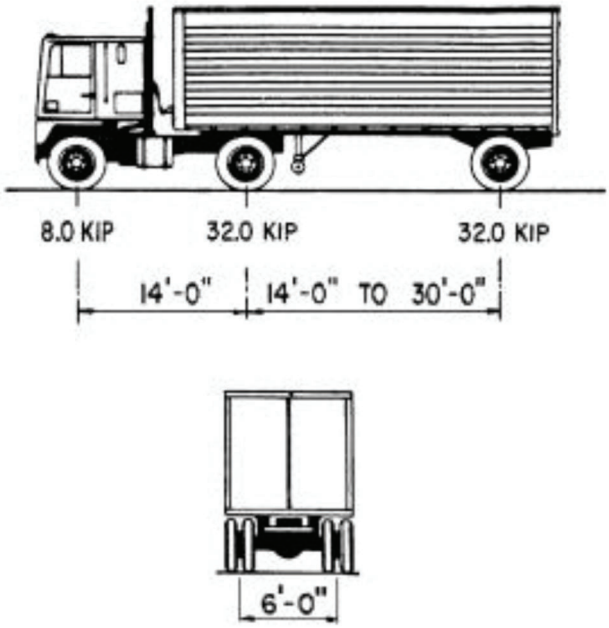

Figure 2.4 LRFR design truck configuration (AASHTO, 2002).

2.3.3 Different Live Load Factors

Live load factors for LRFR and LFR methods are defined differently. Difference in load factors leads to a difference in the rating factors for these methods. LFR uses fixed values of factors i.e., 2.17 for inventory and 1.3 for operating rating. In LRFR, for inventory rating, the live load factor used is 1.75 while for operating rating, 1.35 is used for Strength I limit state design rating (AASHTO, 2018). Joy (2011) showed in his research that the LFR and LRFR rating factors at inventory level are comparable due to LFR load factor of 2.17 being higher than LRFR load factor of 1.75. This leads to balancing the difference generated between LRFR and LFR load effects as HL93 loading is primarily larger than HS20 loading as seen in Section 2.3.1. At operating level, the live load factor for LFR is 1.3, and for LRFR it is 1.35. Since the LFR value is smaller than the LRFR load factor, the same trend is not observed here and the difference in the rating factors increases. The live load factors used in LRFR methodology depend on the rating level, type of vehicle and bridge ADTT (Lichtenstein Consulting Engineers, Inc., 2001). The ADTT of the bridge affects the live load factor as seen in Table 2.1a and 2.1b.

Lichtenstein Consulting Engineers (2001) conducted design and legal load rating for 37 bridges for a comparative study at both inventory and operating levels using the live load factors as discussed above. It was observed that LRFR generated lower rating factors than LFR for both inventory and operating rating. Thus, it was concluded that there are inherent differences in the live load factors between both the methodologies and LRFR produces lower rating factors when compared with LFR.

2.3.4 Difference in Load Combinations

The load combinations used in LFR and LRFR methodologies are essentially different. The different load combinations that are used in the LFR methodology fall under two categories: Service Load Design and Load Factor Design (AASHTO, 2002). For the LRFR methodology, the associated load combinations are calibrated depending on these categories: strength, service, and fatigue limit states (AASHTO, 2020). The load factors corresponding to LFR load combinations are not calibrated and are determined by a "tried and true approach" (Sivakumar, 2007) whereas LRFR load factors are calibrated based on the loading conditions and the examined limit state (Minervino et al., 2004).

TABLE 2.1
Live Load Factors as a Function of ADTT (AASHTO, 2018)

(a) Routine Commercial Traffic	
Traffic Volume (one direction)	Load Factor
Unknown	1.45
ADTT ≥ 5,000	1.45
ADTT ≤ 1,000	1.30
(b) Specialized Hauling Vehicles	
Traffic Volume (one direction)	Load Factor
Unknown	1.45
ADTT ≥ 5,000	1.45
ADTT = 1,000	1.30

2.3.5 Difference in Dynamic Load Allowance

The *LRFD Bridge Design Specifications* (AASHTO, 2020) mention fixed values of impact for different limit states to be used in LRFR, which is 15% for the fatigue and fracture limit state and 33% for most other limit states. In LFR, impact factor is calculated through an expression, and it depends on the span length of the bridge. The expression is given as,

$$I = \frac{50}{L + 125} \qquad \text{(Equation 2.3)}$$

where L (ft.) is the span length.

LRFR accounts for the condition of the bridge roadway like deck joints, cracks, potholes etc., but LFR impact factor is independent of the state of the riding surface. Impact factor, or dynamic load allowance, is not considered for lane loading in LRFR method. In the LFR method, impact is considered for both truck as well as lane load.

2.3.6 Difference in Rating Levels

Another difference between the LFR and LRFR methodologies is the difference in the levels of evaluation of the bridges in each category. Each level of evaluation or rating represents a different level of safety. A two-level system is used by LFR whereas LRFR uses a three-level system. The two-level system of the LFR methodology consists of inventory rating and operating rating while the three-level system used in LRFR methodology comprises of design, legal and permit levels of rating. As seen in Section 2.3.3, the results are comparable for the inventory rating and the difference between the two methodologies increases in the operating level of rating. Since the bridges that were designed by LFD and ASD and are rated with LRFR, inventory level ensures a smooth shift from LFR to LRFR. Operating level load rating is more conservative for LRFR, and it imposes a higher control on the traffic, therefore decreasing the fatigue effects in the members, and leading to a reduction in the maintenance costs. However, it can also lead to higher possibilities of load posting (Joy, 2011).

2.3.7 Difference in Capacity

The deteriorated capacity of a member can be computed and subsequently utilized in both LRFR and LFR. Moreover, LRFR also introduces some reduction factors which accommodate conditions such as traffic volume on the bridge, the redundancy of the superstructure and the growing uncertainty in the

structural capacity resulting from a deteriorating structure (Moen & Fernandez, 2009). The LFR methodology, on the other hand, does not utilize any resistance factors accounting for reduced capacity due to deterioration. However, the LRFR reduction factors result in a reduced capacity of the structure which in turn leads to a smaller rating factor. "The condition φ_c, and system φ_s, resistance factors have been incorporated into LRFR based upon the findings of NCHRP report 301 (Moses & Verma, 1987) and NCHRP Report 406 (Ghosn & Moses, 1998) respectively."

The condition factor, φ_c, considers the reduction in the member capacity due to deterioration of the members. An existing member can undergo deterioration which can lead to an increase in the uncertainties in the capacity and the resistance factor takes that into consideration (Minervino et al. 2004). Moreover, Murdock (2009) reports that, "While the condition factor is related to the structural condition of a member, it only accounts for deterioration from natural causes, such as corrosion, and not from incident-oriented damage." The values of φ_c are shown in Table 2.2.

It is seen that the difference in the rating factors between LFR and LRFR is more for $\varphi_c = 0.85$ than for $\varphi_c = 1.0$, thus concluding that the condition factor can significantly influence the capacity of the member.

The superstructure is made up of different elements or members which interact with each other to make up the entire superstructure. When an element or a member in the superstructure fails or deteriorates, the capacity of the structural system to resist loads is denoted by the bridge's redundancy. The system factor, or φ_s, is a multiplier that accounts for the redundancy of the superstructure (Minervino et al., 2004). The values of φ_s are shown in Table 2.3. Note that lower values correspond to conditions where there is less redundancy than conditions with high φ_s values. The values of φ_c and φ_s change from 0.85 to 1.0, and the manual requires that $\varphi_c\varphi_s \geq 0.85$.

TABLE 2.2
Condition Factor: φ_c (AASHTO, 2018)

Structural Condition of Member	φ_c
Good or Satisfactory	1.00
Fair	0.95
Poor	0.85

TABLE 2.3
System Factor: φ_c (AASHTO, 2018)

Superstructure Type	φ_c
Welded Members in Two-Girder/Truss/Arch Bridges	0.85
Riveted Members in Two-Girder/Truss/Arch Bridges	0.90
Multiple Eyebar Members in Truss Bridges	0.90
Three-Girder Bridges with Girder Spacing 6 ft.	0.85
Four-Girder Bridges with Girder Spacing $\leq$ 4 ft.	0.95
All Other Girder Bridges and Slab Bridges	1.00
Floorbeams with Spacing $>$ 12 ft. and Noncontinuous Stringers	0.85
Redundant Stringer Subsystems between Floorbeams	1.00

2.3.8 Difference in Posting procedures

LFR and LRFR methodology follow different procedures used for posting of bridges. The posting procedures in the LFR methodology relies on the bridge owner's posting procedures. It shall be required to post the bridge if the legal load exceeds the load resistance of the bridge at operating level as noted in the MBE (AASHTO, 2018). LRFR methodology also permits the bridge owner to load post a bridge based on their own posting practices. However, this approach is more systematic than the LFR methodology. If the legal rating factor is more than 1.0, the safe posting load is equivalent to the load capacity (INDOT, 2020). If the rating factor lies between 0.3 and 1.0, a safe posting load is calculated using the following equation as mentioned in MBE (AASHTO, 2018).

$$\text{Safe Posting Load} = \frac{W}{0.7}[(RF) - 0.3] \quad \text{(Equation 2.4)}$$

Where, RF is the legal load rating factor and W is the weight of the rating vehicle.

If the rating factor is lower than 0.3, then that type of vehicle should not be allowed to travel across the bridge. It is up to the bridge owner to decide when to shut down a bridge, but the MBE (AASHTO, 2018) indicates that the bridges which cannot carry a live load of three tons must cease to operate. Research done previously confirms that the posting loads corresponding to LRFR are found to be notably lower than the ones based on LFR methodology (Murdock, 2009).

2.4 AASHTOWare BrR

This research was based on extensive use of AASHTOWare BrR (Version 7.0) along with SAP2000 and Mathcad to perform separate checks. Apart from the constant guidance by Jennifer Hart at the Indiana Department of Transportation (INDOT), there were several resources that were utilized to

acquire a basic understanding of AASHTOWare BrR. The *BrR Load Rating Tools and Tips* (United Consulting, 2016) was referred for obtaining knowledge about the fundamentals of AASHTOWare BrR. Features such as creating the model and generating output were explored. This research did not require the creation of the models since the bridge files were provided by INDOT to the research team. This resource was used for learning the steps to generate the output after running the analysis. Various features such as the report tool, spec check, and analysis output were introduced in this article which were deployed for analyzing the rating results in depth.

It will be later seen in Section 3.3, that a feature called "Capacity Override" is used to modify the value of the capacity of the member. The article *AASHTOWare Bridge Design and Rating Training* (AASHTO, 2013) was used to learn about overriding the capacity at the points of interest. This article was used as a guide to change the capacity value of the member and the steps to proceed will be shown through screenshots in Section 3.3.

AASHTOWare BrR uses the provisions of the *LRFD Bridge Design Specifications* (AASHTO, 2020) to auto calculate the live load distribution factors. The user can also modify the live load distribution factors by inserting the values calculated separately, and Section 4.3 discusses that feature. The *CTDOT BrR User Guide* (CTDOT, 2018) mentions the live load distribution factor overrides and how it can be used. The *AASHTOWare BrR Workarounds* (Ward, 2019) presented a method to change the AASHTO range of applicability which can also be employed to avoid the calculation of live load distribution factor by the lever rule.

3. LATERAL TORSIONAL BUCKLING

3.1 Overview

Lateral torsional buckling is a phenomenon which involves both lateral displacement as well as twisting of the member. This situation occurs in beams where the compression flange is free to move in a lateral direction as well as undergo rotation. Such beams, or portions of beams are referred to as unrestrained beams. The flanges under compression need to be restrained to prevent the occurrence of lateral torsional buckling. The two major processes in lateral torsional buckling are explained in detail below.

Lateral Deflection

When a vertical load is applied to a beam, compression occurs in one flange and tension in the other. Due to this, the flange under compression attempts to deflect laterally, whereas the tension flange tries to resist this motion and keep the member straight. This lateral deflection causes the generation of restoring forces which try to keep the member straight. These restoring forces along with the lateral component of the tensile forces control the member's buckling resistance (NSC2, 2006).

Torsion

As mentioned earlier, apart from lateral deflection of the beam, twisting of the member is also involved in lateral torsional buckling. The resistance to twisting is determined by the torsional stiffness of the member. The thickness and the width of the flange influences the torsional stiffness of the member. A section with thicker flanges has a larger bending strength as compared to the one with thinner flanges with the same overall depth (NSC2, 2006).

3.1.1 Factors Affecting Lateral Torsional Buckling

3.1.1.1 Location of the applied load. The location of the load is a major factor which affects lateral torsional buckling. The distance measured vertically between the point of load application and the shear center of the section determines the vulnerability of the section to lateral torsional buckling effects. The susceptibility to lateral torsional buckling increases if the point of load application is above the shear center. On the other hand, if the load is applied through or below the shear center, the effects due to lateral torsional buckling are reduced (NSC2, 2006).

3.1.1.2 Shape of the applied bending moment. The resistance to lateral torsional buckling is affected by the shape of the bending moment acting on the beam. If the bending moment is non-uniform over the member length, the member is less susceptible to the effects of lateral torsional buckling. The buckling resistance is higher as compared to when uniform bending moment of the same intensity is applied on the member (NSC2, 2006). The moment gradient factor defines the change in bending moment throughout the member. When the value of the moment gradient factor is 1.0, it signifies uniform bending moment throughout the section. Moment gradient is an important topic of discussion for this research, and it will be described further in the sections that follow.

3.1.1.3 End support conditions. The resistance to lateral torsional buckling is directly proportional to the lateral and rotational restraint in the end supports. For end conditions which provide more restraint to the member, the buckling resistance increases and vice versa (NSC2, 2006). In general, lateral torsional buckling is affected by the slenderness of the section. The length of the beam, lateral bending stiffness of the flanges and the torsional stiffness of the member are the controlling factors for this limit state. The following sections discuss the equations that are used to compute the lateral torsional buckling resistance for LFD and LRFD methodologies.

3.1.2 Flexural Resistance–LFD

The equations for lateral torsional buckling resistance for Load Factor Design (LFD) are given in 10.48.4 in the *Standard Specifications for Highway Bridges* (AASHTO, 2002) and are explored in this

section. This section discusses the various requirements and equations for partially braced members.

The maximum lateral torsional buckling strength is calculated as,

$$M_u = M_r R_b \qquad \text{(Equation 3.1)}$$

where, R_b is the flange-stress reduction factor. The value of R_b is equal to 1 for longitudinally stiffened girders if:

$$\frac{D}{t_w} \le 5{,}460\sqrt{\frac{k}{f_b}} \qquad \text{(Equation 3.2)}$$

where,

$$\text{for } \frac{d_s}{D_c} \ge 0.4 \; k = 5.17\left(\frac{D}{d_s}\right)^2 \ge 9\left(\frac{D}{D_c}\right)^2$$

$$\text{for } \frac{d_s}{D_c} < 0.4 \; k = 11.64\left(\frac{D}{D_c - d_s}\right)^2$$

Here d_s is the distance from the centerline of a plate longitudinal stiffener to the inner surface, D is the clear distance between the flanges and f_b is the factored bending stress in the compression flange.

For girders with or without longitudinal stiffeners, R_b is computed as,

$$R_b = 1 - 0.002\left(\frac{D_c t_w}{A_{fc}}\right)\left[\frac{D_c}{t_w} - \frac{\lambda}{\sqrt{\frac{M_r}{S_{xc}}}}\right] \le 1.0 \qquad \text{(Equation 3.3)}$$

where D_c is the depth of web in compression (in.), t_w is the thickness of the web (in.), M_r is the lateral torsional buckling moment (lb-in.), S_{xc} is the section modulus with respect to compression flange (in.^{3}), A_{fc} is the area of the compression flange (in.^{2}) and λ is a constant value of 154,000 for all sections where $D_c \le D/2$. λ is equal to 12,500 for sections where $D_c > D/2$.

The lateral torsional buckling resistance, M_r is defined as follows.

For sections with $\frac{D_c}{t_w} \le \frac{\lambda}{\sqrt{F_y}}$ or with longitudinally stiffened webs:

$$M_r = 91 * 10^6 C_b\left(\frac{I_{yc}}{L_b}\right)\sqrt{0.772\frac{J}{I_{yc}} + 9.87\left(\frac{d}{L_b}\right)^2} \le M_y \qquad \text{(Equation 3.4)}$$

For sections with $\frac{D_c}{t_w} > \frac{\lambda}{\sqrt{F_y}}$:

- If $L_b \le L_p$,

$$M_r = M_y \qquad \text{(Equation 3.5)}$$

- If $L_r \ge L_b > L_p$,

$$M_r = C_b F_y S_{xc}\left[1 - 0.5\left(\frac{L_b - L_p}{L_r - L_p}\right)\right] \qquad \text{(Equation 3.6)}$$

- If $L_b > L_r$,

$$M_r = C_b \frac{F_y S_{xc}}{2}\left(\frac{L_r}{L_b}\right)^2 \qquad \text{(Equation 3.7)}$$

Where, L_b is the unbraced length of the compression flange (in.), L_p is the limiting plastic unbraced length (in.) and is equal to,

$$L_p = 9{,}500\, r'/\sqrt{F_y} \qquad \text{(Equation 3.8)}$$

where r' is the radius of gyration (in.) of the compression flange about the vertical axis in the plane of the web.

L_r is the limiting unbraced length for elastic behavior (in.) and is equal to,

$$L_r = \left(\frac{572 * 10^6 I_{yc} d}{F_y S_{xc}}\right)^{1/2} \qquad \text{(Equation 3.9)}$$

M_y is the yield moment (lb-in.), I_{yc} is the moment of inertia of the compression flange about the vertical axis in the plane of the web (in.^{4}), d is the depth of the girder (in.), J is the polar moment of inertia (in.^{3}) given by,

$$J = \frac{(bt^3)_c + (bt^3)_t + D{t_w}^3}{3} \qquad \text{(Equation 3.10)}$$

where b (in.) and t (in.) are the width and the thickness of the compression and tension flange, respectively.

C_b is called the bending coefficient in LFD methodology and is calculated as,

$$C_b = 1.75 + 1.05\left(\frac{M_1}{M_2}\right) + 0.3\left(\frac{M_1}{M_2}\right)^2 \le 2.3 \qquad \text{(Equation 3.11)}$$

Here M_1 is the smaller moment end moment and is the larger end moment within the unbraced length. The ratio of M_1/M_2 is taken to be positive for reverse curvature and negative for single curvature. C_b is taken equal to 1.0 for unbraced cantilevers and for sections in which the moment within the unbraced length is greater or equal to the larger of the end moments (M_2).

3.1.3 Flexural Resistance–LRFD

3.1.3.1 General. The flexural resistance of composite sections in negative flexure and non-composite sections by LRFD methodology is discussed in 6.10.8 in the *LRFD Bridge Design Specifications* (AASHTO, 2020). As seen in the previous section for LFD, the lateral torsional buckling resistance of members are presented in terms of a "moment" value. In the LRFD methodology, the resistance values are indicated as a "stress" value.

The following sections discuss the requirements that need to be satisfied in the case of discretely or continuously braced flanges.

3.1.3.1.1 Discretely braced flanges in compression. Flanges that are discretely braced in compression

need to satisfy the following requirement for the strength limit state.

$$f_{bu} + \frac{1}{3} f_l \leq \phi_f F_{nc}$$

Where, f_{bu} is the largest value of compressive stress throughout the unbraced length in the flange under consideration, calculated without consideration of flange lateral bending (ksi), f_l is the largest value of flange lateral bending stress throughout the unbraced length in the flange under consideration (ksi), f_{nc} is the nominal flexural resistance of the compression flange (ksi), φ_f is the resistance factor for flexure, i.e., $\varphi_f = 1.00$.

3.1.3.1.2 Discretely braced flanges in tension. For flanges discretely braced in tension, the following requirement needs to be satisfied for strength limit state.

$$f_{bu} + \frac{1}{3} f_l \leq \phi_f F_{nt}$$

Where, F_{nt} is the nominal flexural resistance of the tension flange (ksi)

3.1.3.1.3 Continuously braced flanges in tension or compression. Flanges that are continuously braced in tension or compression shall satisfy the following requirement for strength limit

$$f_{bu} \leq \phi_f R_h F_{yf}$$

Where, F_{yf} is the specified minimum yield strength of the flange (ksi), R_h is the hybrid factor. For rolled shapes, homogenous built-up sections, and built-up sections with a higher-strength steel in the web than in both flanges, R_h is taken as 1.0. For the members evaluated in this research, the sections are homogenous and therefore, R_h is taken as equal to 1.0.

It should be noted that f_{bu} and f_l in the above equations are based on factored loads and shall always be taken as positive in all the equations.

3.1.3.2 Flexural resistance–compression flange. The lateral torsional buckling resistance of the compression flange is calculated according to 6.10.8.2.3 in the *LRFD Bridge Design Specifications* (AASHTO, 2020). The expressions used for buckling resistance vary according to the value of the unbraced length. The expressions shown below are valid for a prismatic section.

If $L_b \leq L_p$,

$$F_{nc} = R_b R_h F_{yc} \qquad \text{(Equation 3.12)}$$

If $L_p < L_b \leq L_r$,

$$F_{nc} = C_b \left[1 - \left(1 - \frac{F_{yr}}{R_h F_{yc}} \right) \left(\frac{L_b - L_p}{L_r - L_p} \right) \right] \qquad \text{(Equation 3.13)}$$

$$R_b R_h F_{yc} \leq R_b R_h F_{yc}$$

If $L_b > L_r$,

$$F_{nc} = F_{cr} \leq R_b R_h F_{yc} \qquad \text{(Equation 3.14)}$$

Where, is the unbraced length (in.), is the limiting unbraced length to achieve the nominal flexural resistance of $R_b R_h F_{yc}$ under uniform bending (in.). L_p is given by,

$$L_p = 1.0\ r_t \sqrt{\frac{E}{F_{yc}}} \qquad \text{(Equation 3.15)}$$

L_r is the limiting unbraced length to achieve the onset of nominal yielding in either flange under uniform bending with consideration of compression flange residual stress effects (in.). L_r is given by,

$$L_r = \pi r_t \sqrt{\frac{E}{F_{yr}}} \qquad \text{(Equation 3.16)}$$

R_b is the web load-shedding factor, F_{yc} is specified minimum yield strength of the compression flange (ksi), F_{yr} is the compression flange stress at the onset of nominal yielding within the cross section, including residual effects but not including compression flange lateral bending, taken as smaller of 0.7 F_{yc} and F_{yw}, but not less than 0.5 F_{yc} (ksi).

F_{cr} is the elastic lateral-torsional buckling stress (ksi). F_{cr} is given as,

$$F_{cr} = \frac{C_b R_b \pi^2 E}{\left(\frac{L_b}{r_t} \right)^2} \qquad \text{(Equation 3.17)}$$

Where, r_t is the effective radius of gyration for lateral torsional buckling (in.) and is given by,

$$r_t = \frac{b_{fc}}{\sqrt{12 \left(1 + \frac{1}{3} \frac{D_c t_w}{b_{fc} t_{fc}} \right)}} \qquad \text{(Equation 3.18)}$$

Where, b_{fc} is the effective width of the compression flange (in.), D_c is the depth of the web in compression in the elastic range (in.), t_w is the thickness of the web (in.), t_{fc} is the thickness of the compression flange (in.), C_b is moment gradient factor or modifier. The calculation of C_b is explained below.

- For unbraced cantilevers and where $\frac{f_{mid}}{f_2} > 1$ or $f_2 = 0$

$$C_b = 1.0 \qquad \text{(Equation 3.19)}$$

- For all other cases:

$$C_b = 1.75 - 1.05 \left(\frac{f_1}{f_2} \right) + 0.3 \left(\frac{f_1}{f_2} \right)^2 \leq 2.3 \qquad \text{(Equation 3.20)}$$

Where, f_{mid} is the stress at the middle of the unbraced length of the flange under consideration without consideration of lateral bending, calculated from the moment envelope value that produces largest compres-

sion at this point, or smallest tension if the point is never in compression (ksi), f_2 is the largest compressive stress at either end of the unbraced length of the flange under consideration without considering lateral bending, calculated from the critical moment envelope value (ksi), f_0 is the stress at the brace point opposite to the one corresponding to f_2 without considering lateral bending, calculated from the moment envelope value that produces largest compression at this point, or smallest tension if the point is never in compression (ksi), f_1 is the stress at the brace point opposite to the one corresponding to f_2 without considering lateral bending. It is calculated as the intercept of the most critical assumed linear stress variation passing through f_2 and either f_{mid} or f_0, whichever produces the smaller value of C_b (ksi).

The following points may be taken in mind to calculate f_1:

- When the variation in the moment along the entire length between the brace points is concave in shape:

$$f_1 = f_0 \qquad \text{(Equation 3.21)}$$

- Otherwise:

$$f_1 = 2f_{mid} - f_2 \geq f_0 \qquad \text{(Equation 3.22)}$$

Appendix C6 in the *LRFD Bridge Design Specifications* (AASHTO, 2020) gives a detailed explanation for the calculation of C_b which are shown in Figure 3.1.

An important fact to remember is that these calculations and examples shown above assume a prismatic section, i.e., the member cross section remains constant throughout the unbraced length. These calculations are also valid for non-prismatic sections if the transition to the smaller section lies within 20% of the unbraced length measured from the brace point with the smaller moment (AASHTO, 2020).

3.1.4 Differences in LTB Equations–LFD and LRFD

Sections 3.1.2 and 3.1.3 present the equations used for lateral torsional buckling in the LFD and LRFD methodologies, respectively. It can be observed that there are some fundamental differences between the two approaches. These differences are discussed further in this section.

The limiting unbraced lengths L_p and L_r are defined differently in the LFD and LRFD specifications as seen in Equations 3.8, 3.9, and 3.15, 3.16, respectively.

Another major difference between the two methodologies for the limit state of lateral torsional buckling is the calculation of C_b. LFD defines C_b as the bending coefficient whereas LRFD calls it as the moment gradient modifier. The equations used for the calculation for the two approaches are also different. Equations 3.11 and 3.20 are listed again for comparison,

$$C_b = 1.75 + 1.05\left(\frac{M_1}{M_2}\right) + 0.3\left(\frac{M_1}{M_2}\right)^2 \leq 2.3 \text{ (LFD)}$$

$$C_b = 1.75 - 1.05\left(\frac{f_1}{f_2}\right) + 0.3\left(\frac{f_1}{f_2}\right)^2 \leq 2.3 \text{ (LRFD)}$$

It is evident that for both LFD and LRFD, the upper-bound for C_b is 2.3. While LFD uses the end moments, M_1 (smaller) and M_2 (larger) in the equation, LRFD uses the concept of the intercept of the linear stress variation passing through f_2 (larger) and either f_{mid} or f_0 (smaller), depending on the one that generates a more critical value of C_b. Thus, the basic concepts for the calculation of C_b are rather different. The way that these two methodologies treat non-prismatic sections is also significantly different. According to the LRFD if the member is non-prismatic within the unbraced length, then C_b is taken as 1.0. LFD, on the other hand, does not consider if the member is prismatic or non-prismatic. It assumes the member to be prismatic even though the cross section changes within the unbraced length, and the resulting C_b value comes out to be greater than 1.0.

The expressions for the calculation of lateral torsional buckling capacity are different for these two methodologies as seen in the equations above.

A striking difference between the calculation of the capacities in the LFD and LRFD methodology is related to the St. Venant torsional constant, J. It is assumed to be equal to zero for the capacity calculations in LRFD as it was seen in Equation 3.17,

$$F_{cr} = \frac{C_b R_b \pi^2 E}{\left(\frac{L_b}{r_t}\right)^2}$$

The commentary in the *LRFD Bridge Design Specifications* (AASHTO, 2020) explains that it is wise and convenient to assume J as equal to zero for cases like longitudinally stiffened girders with web slenderness approaching the maximum limit. The LRFD methodology suggests that in such cases, the contribution of J to the lateral torsional buckling capacity is negligible and it can be ignored. On the other hand, LFD methodology includes the torsional constant, J in the expression for the lateral torsional buckling capacity for the girders with longitudinal stiffeners as seen in Equation 3.4.

$$M_r = 91 * 10^6 C_b \left(\frac{I_{yc}}{L_b}\right) \sqrt{0.772\frac{J}{I_{yc}} + 9.87\left(\frac{d}{L_b}\right)^2} \leq M_y$$

The difference generated due to this additional constant in the capacity equations leads to the capacity being slightly higher for LFD methodology, and although the difference is very small, it still is another reason for the LRFD capacity being lesser than LFD capacity and rating factors being lower for LRFD methodology.

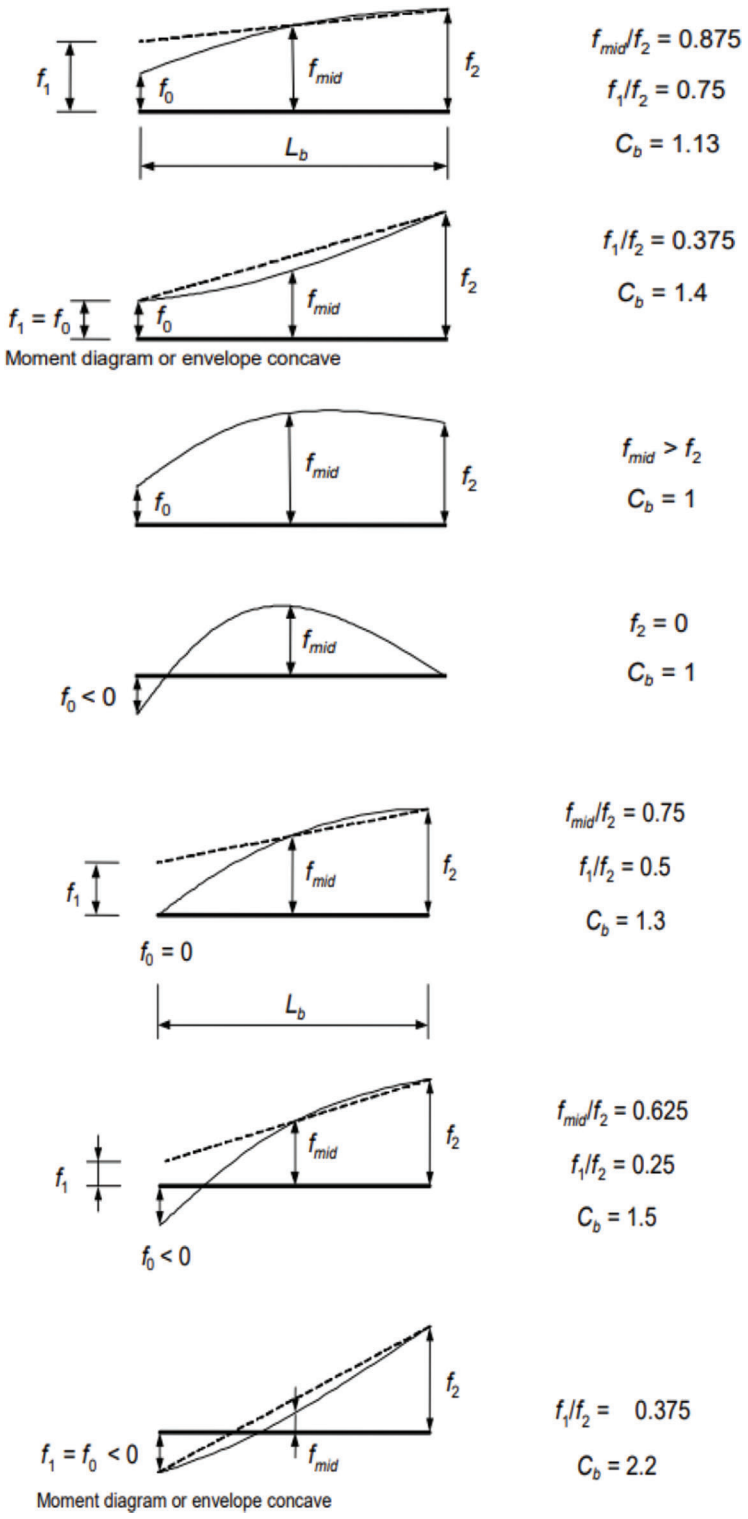

Figure 3.1 C_b calculation–LRFD (AASHTO, 2020).

These differences as stated above result in the differences between the values of the lateral torsional buckling capacities of the member by LFD and LRFD methods. The differences in the capacities further lead to variations in the rating values produced by these two methodologies.

3.2 Observations and Comparisons–AASHTOWare BrR and SAP2000

A few bridges were identified by INDOT which produced rating factors less than 1 for the limit state of lateral torsional buckling by the LRFR methodology.

However, these bridges were rating more than one for the LFR methodology. The rating calculations were carried out using the AASHTOWare BrR software.

INDOT provided these bridges for further examination in AASHTOWare BrR. A list of these bridges along with various characteristics such as number of spans, span lengths, web depth, steel rolled shapes, composite or non-composite (C/NC), and skew angle are provided in Table 3.1.

A structural analysis is conducted for specified vehicle loadings when running the AASHTOWare BrR software. However, to perform a separate and independent check on the BrR calculations, a separate analysis was carried out using SAP2000 to calculate the dead load and live load moments and shears acting on the girders. The capacity and subsequently the rating factors were then computed separately using Mathcad. The results from SAP2000 and Mathcad were then compared to AASHTOWare BrR results in order to determine whether or not BrR results are credible and propose some recommendations to resolve the issue of discrepancies between the different methodologies.

The observations made from the comparisons of these two evaluations for lateral torsional buckling are examined in the sections that follow.

3.2.1 Comparisons with AASHTOWare BrR Results

3.2.1.1 SAP2000 analysis. SAP2000 was used to conduct a separate analysis to calculate the dead load and live load moments and shears acting on the girder. The results were then compared with the moments and shears produced in the AASHTOWare software. All the bridges provided by INDOT were modelled in SAP2000 to calculate the moments and shears. The evaluation of one such bridge is shown for illustration purposes.

3.2.1.1.1 INDOT Str. No. (Bridge ID): 009-30-06644. As seen in the Table 3.1, this is a 3-span continuous non-composite bridge with span lengths 56 ft., 71 ft., and 56 ft. A SAP2000 model was constructed using beam elements with these span lengths. The plan view, framing plan and the typical cross section of the bridge are shown in Figures 3.2, 3.3, and 3.4, respectively.

An elevation view of the girder is shown in Figure 3.5.

3.2.1.1.2 Dead load effects. After the model was assembled, loads were assigned. The values of the calculated dead loads are shown below in Table 3.2. The weight of the deck, railings, beam weight and haunch were used to calculate a uniform dead load.

These dead loads were assigned to the beam and the analysis was run. The moments and shear values due to the dead loads at every 10th point are tabulated below in Tables 3.3 and 3.4, respectively. Along with the SAP2000 results, the tables also show the values produced by AASHTOWare BrR. This was done in order to draw comparisons between SAP2000 and AASHTOWare BrR analysis. It can be seen from the two tables that the dead load moment and shear results generally agree very well; some anomalies were observed, however, in the BrR results near regions where section changes occur.

These values are then plotted as shown in Figures 3.6 and 3.7 for moments and shears, respectively.

TABLE 3.1
Bridge Characteristics–Lateral Torsional Buckling

No.	INDOT Str. #	No. of Spans	Span Length (ft.)	Web Depth (in.)	Beam Size	C/NC	Skew (deg.)
1.	025-09-06941	3	95, 114, 95	38	–	C	Varies
2.	I70-008-02344 BWBL	4	58.75, 75.25, 75.25, 58.75	–	W30 × 116/ W30 × 108	C	41.975
3.	I465-131-07719 A	2	150, 150	52 and 52-72 (varies)	–	C	0
4.	I70-079-02420 E	3	150, 150, 120.42	68	–	NC	0
5.	912-45-06599	3	40, 60.5, 40	–	W30 × 99/ W30 × 108	NC	13.73
6.	062-13-07329 A	3	97, 121, 97	42	–	C	54.433
7.	0I70-076-02376 B	3	64, 80, 64	–	W33 × 118	C	44.68/2.29 (Lt)
8.	I70-123-02361 JDEB	6	58.067, 58.067, 58.067, 58.067, 71, 58.067	–	W30 × 124/ W30 × 132	C	41.15 (Rt.)
9.	I70-123-02361 DWBL	6	58.067, 58.067, 58.067, 58.067, 71, 58.067,	–	W30 × 124/ W30 × 132	C	41.15 (Rt.)
10.	234-83-07152	5	146, 176, 176, 176, 146	72	–	C	13 (Lt.)
11.	009-30-06644 A	3	56, 71, 56	–	W33 × 118/ W33 × 130	NC	18 (Rt.)
12.	P000-47-07089	3	11.5, 16.0833, 11.5	–	W10 × 22	NC	40 (Lt.)
13.	049-64-06679 CNBL	3	36, 86, 32	42	W24 × 76/ W24 × 68	C	0
14.	049-64-06679 CSBL	3	36, 86, 32	42	W24 × 76/ W24 × 68	C	0

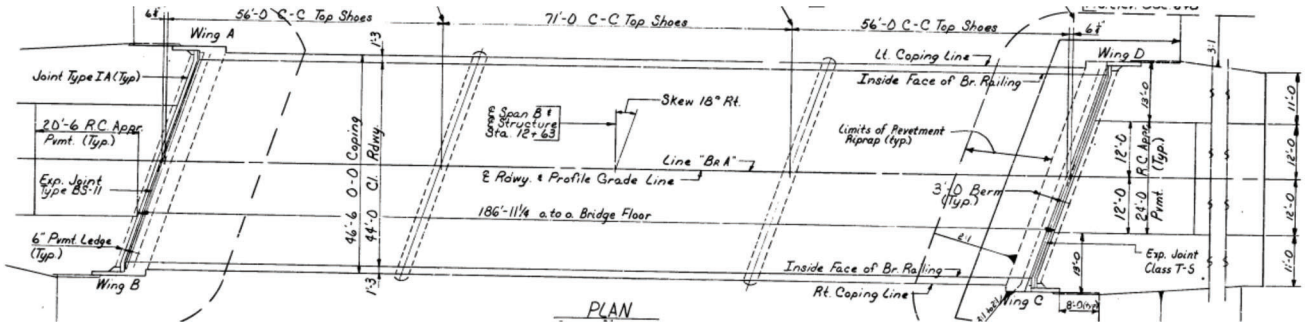

Figure 3.2 Plan view 009-30-06644 (J. Hart, personal communication, January 2020).

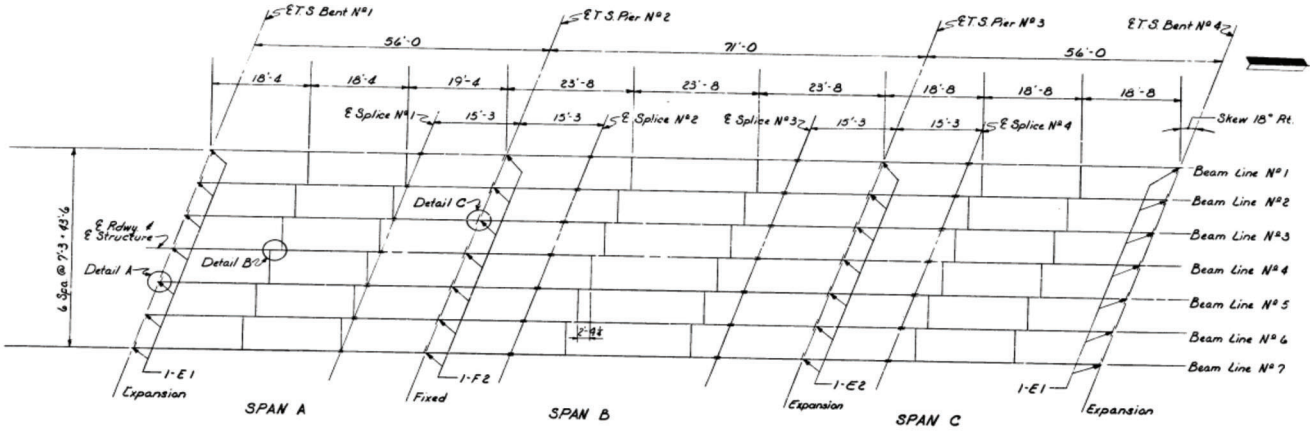

Figure 3.3 Framing plan 009-30-06644 (J. Hart, personal communication, January 2020).

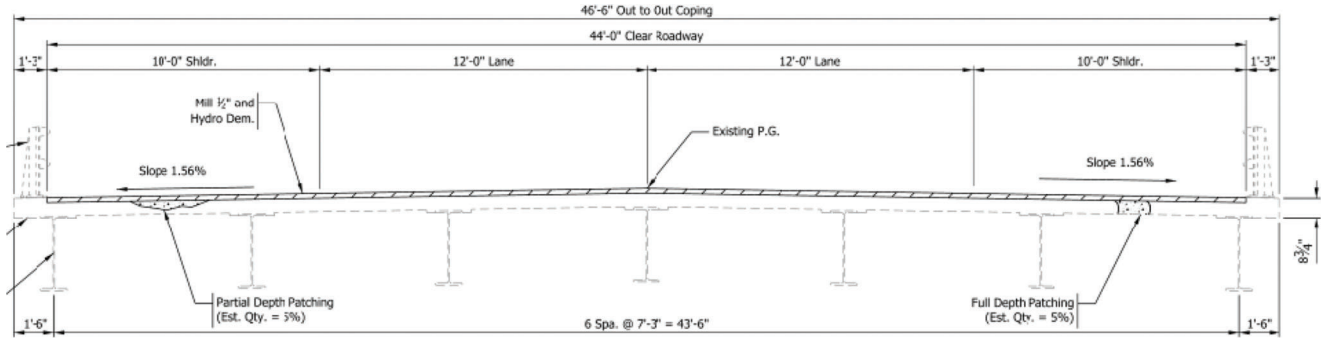

Figure 3.4 Typical cross section 009-30-06644 (J. Hart, personal communication, January 2020).

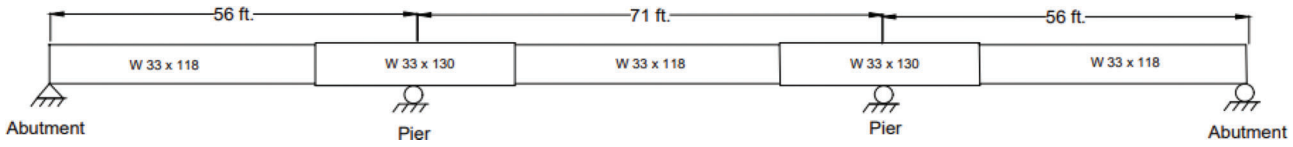

Figure 3.5 Girder elevation 009-30-06644.

It can be observed from Figures 3.6 and 3.7 that the dead load moments and shears calculated by SAP2000 and AASHTOware BrR are very comparable for this bridge.

3.2.1.1.3 Live load effects. The legal loads that are used for carrying out live load analysis depend on the vehicles prescribed by AASHTO plus the respective manual for each state in the country. The legal loads used in the state of Indiana comprise of the vehicles mentioned in *The Manual of Bridge Evaluation* (AASHTO, 2018) and the *INDOT Bridge Inspection Manual* (INDOT, 2020). The LRFR legal loads used are shown in Table 3.5.

The configurations of the AASHTO vehicles are illustrated in the MBE (AASHTO, 2018) and they are

TABLE 3.2
Dead Load Effects on Exterior Beam

Load Type	Uniform Load Per Unit Length (kip/ft.)
Deck	0.577
Railings	0.008
Self-weight	0.121 (Spans 1 & 3) 0.123 (Span 2)
Haunch	0.010

TABLE 3.3
Comparison of Dead Load Moments

Moment		
Station	**SAP2000**	**AASHTOWare BrR**
ft	**Kip-ft**	**Kip-ft**
0	0.00	0
5.6	71.64	70.7
11.2	120.82	118.98
16.8	147.54	144.83
22.4	151.79	148.26
28	133.58	129.26
33.6	92.91	70.7
39.2	29.78	24
44.8	-55.81	-62.38
50.4	-163.87	-138.04
56	-294.39	-303.59
0	-294.39	-303.59
7.1	-131.48	-140.31
14.2	-4.77	-13.72
21.3	85.74	76.4
28.4	140.04	130.47
35.5	158.14	148.5
42.6	140.04	105
49.7	85.74	76.4
56.8	-4.77	-13.72
63.9	-131.48	-112.99
71	-294.39	-303
0	-294.39	-303.59
5.6	-163.87	-171.57
11.2	-55.81	-62.38
16.8	29.78	24
22.4	92.91	87.84
28	133.58	129.26
33.6	151.79	119.46
39.2	147.54	144.83
44.8	120.82	118.98
50.4	71.64	56.99
56	0.00	0

defined accordingly in SAP2000. SAP2000 uses the feature of "Moving Load" to carry out the application of the live load for the analysis. The steps used in SAP2000 for live load analysis are described below. For this example, the analysis results for the AASHTO SU7 vehicle is shown.

1. Defining the Path
   The first step for live load analysis is to define the path for the vehicle. The vehicle goes over all the three spans and therefore the path here includes frames 1, 2, and 3.

TABLE 3.4
Comparison of Dead Load Shears

Shear		
Station	**SAP2000**	**AASHTOWare BrR**
ft	**Kip**	**Kip**
0	14.80	14.63
5.6	10.79	10.62
11.2	6.78	6.62
16.8	2.77	2.61
22.4	-1.25	-1.39
28	-5.26	-5.39
33.6	-9.27	-7.58
39.2	-13.28	-13.4
44.8	-17.29	-17.46
50.4	-21.30	-17.27
56	-25.31	-25.61
0	25.50	25.58
7.1	20.40	20.41
14.2	15.30	15.24
21.3	10.20	10.15
28.4	5.10	5.08
35.5	0.00	0
42.6	-5.10	-4.09
49.7	-10.20	-10.15
56.8	-15.30	-15.24
63.9	-20.40	-16.37
71	-25.50	-25.58
0	25.31	25.61
5.6	21.30	21.54
11.2	17.29	17.46
16.8	13.28	13.4
22.4	9.27	9.4
28	5.26	5.39
33.6	1.25	1.12
39.2	-2.77	-2.61
44.8	-6.78	-6.62
50.4	-10.79	-8.56
56	-14.80	-14.63

2. Defining the Vehicle
   This configuration of the truck was defined in the MBE (AASHTO, 2018) and uploaded into SAP2000 by selecting the feature "Define Vehicles" and adding the axle loads and the axle spacings as shown in Figure 3.8.
3. Defining Load Pattern and Load Case
   The load pattern is set as "Vehicle Live" and the load case as "Moving Load." After defining these prerequisites for SAP2000, the analysis is run.

The distribution factors for each span are calculated separately and an impact factor of 1.33 (33%) is utilized. These factors are applied to SAP2000 results and tabulated below in Table 3.6 for moments and Table 3.7 for the shear. The values obtained using AASHTOWare BrR are also listed in the tables.

These values are plotted as shown in Figure 3.9 for moments and Figure 3.10 for shears.

It can be clearly observed that the live load moments and shears calculated using SAP2000 and AASHTOW are BrR are very comparable. The influence lines were produced by SAP2000 at every 10th point and the truck

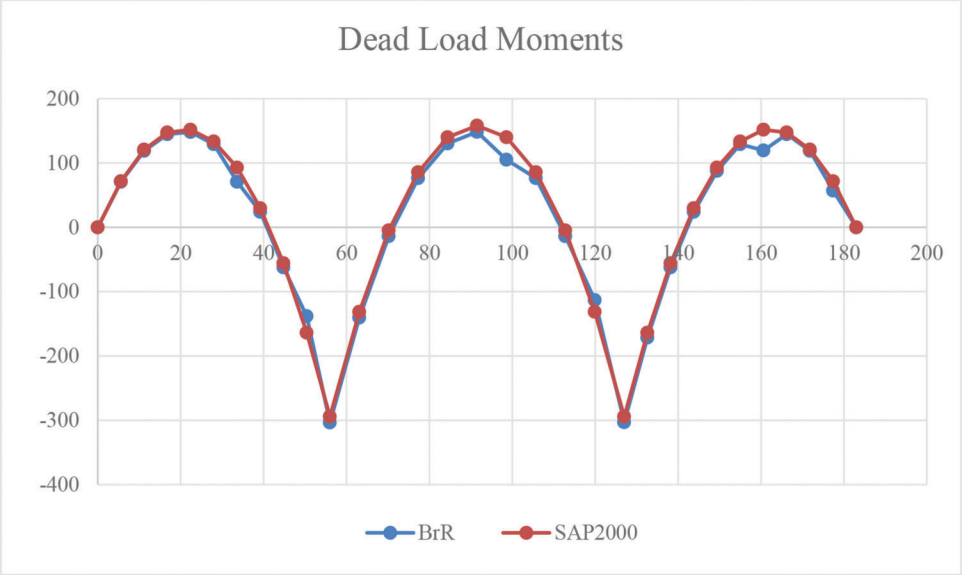

Figure 3.6 Comparison of dead load moments.

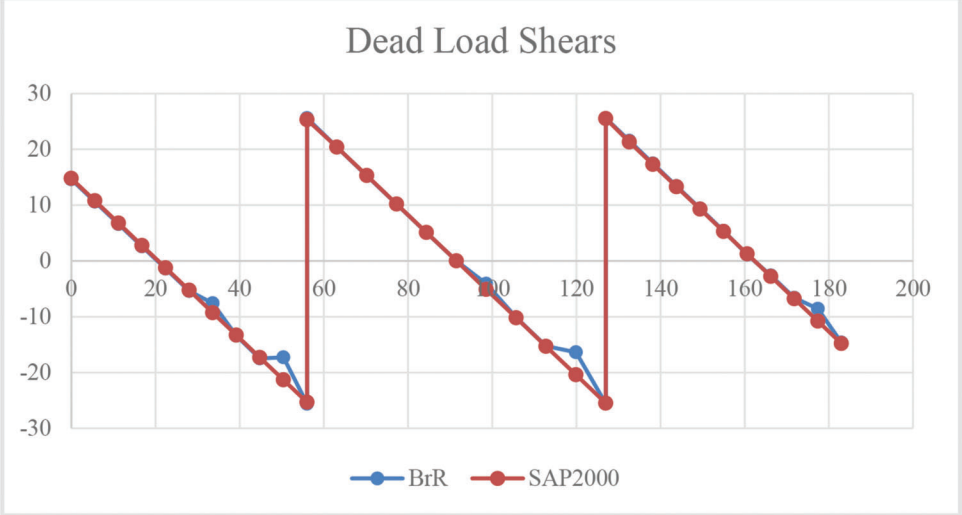

Figure 3.7 Comparison of dead load shears.

TABLE 3.5
Indiana Legal Loads (INDOT, 2020)

Truck Configuration	LRFR Subcategory
H-20	Routine Commercial Traffic
HS-20	Routine Commercial Traffic
Alternate Military	Routine Commercial Traffic
AASHTO Type 3	Routine Commercial Traffic
AASHTO Type 3S2	Routine Commercial Traffic
AASHTO Type 3-3	Routine Commercial Traffic
AASHTO Lane-Type	Routine Commercial Traffic
EV2	Routine Commercial Traffic
EV3	Routine Commercial Traffic
AASHTO NRL	Specialized Hauling
AASHTO SU4	Specialized Hauling
AASHTO SU5	Specialized Hauling
AASHTO SU6	Specialized Hauling
AASHTO SU7	Specialized Hauling

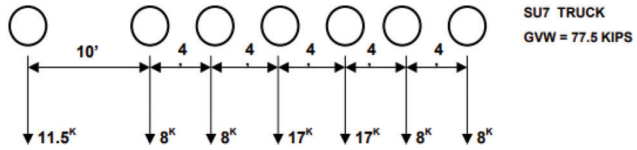

Figure 3.8 SU7 truck (AASHTO, 2018).

was placed manually in such a way that maximum effect was generated at that location.

3.2.1.2 Rating factors calculation–Mathcad. After compiling the moments and shears from SAP2000 analysis, the next step was to calculate the capacity of the member. This was accomplished by creating worksheets in Mathcad. The capacity calculated here is based on the smaller cross section, since BrR considers the

TABLE 3.6
Live Load Effects (Moment)–SU7

	SAP2000		AASHTOWare BrR	
Station	**+ M3**	**- M3**	**+M3**	**-M3**
ft	**Kip-ft**	**Kip-ft**	**Kip-ft**	**Kip-ft**
0.00	0.00	0.00	0.00	0.00
5.60	211.54	-33.96	215.42	-37.48
11.20	376.08	-67.86	381.16	-74.96
16.80	487.50	-101.76	489.76	-112.44
22.40	531.74	-135.67	527.22	-149.91
28.00	529.22	-169.57	518.20	-187.39
33.60	489.57	-203.48	463.370	-224.871
39.20	401.77	-237.38	361.95	-262.35
44.80	271.34	-271.29	216.18	-299.83
50.40	80.41	-390.69	78.921	-337.307
56.00	93.47	-374.79	87.69	-374.99
0.00	93.47	-374.79	87.69	-374.79
7.10	70.35	-272.64	62.5	-261.73
14.20	265.69	-224.00	265.13	-222.92
21.30	428.39	-194.95	420.68	-184.11
28.40	518.91	-156.95	514.27	-145.29
35.50	528.80	-114.95	548.06	-106.62
42.60	496.91	-154.95	514.321	-145.481
49.70	413.39	-194.95	421.20	-184.28
56.80	265.69	-214.00	265.42	-223.20
63.90	82.35	-252.64	61.651	-262.065
71.00	93.47	-374.79	87.58	-374.29
0.00	93.47	-374.79	87.58	-374.29
5.60	85.41	-338.69	78.82	-336.86
11.20	222.34	-287.29	216.24	-299.43
16.80	368.77	-247.38	361.82	-262.00
22.40	471.57	-203.48	463.56	-224.57
28.00	526.22	-179.57	518.26	-187.14
33.60	531.74	-135.67	527.327	-149.716
39.20	487.50	-101.76	489.86	-112.29
44.80	376.08	-67.86	381.15	-74.86
50.40	211.54	-33.96	215.450	-37.429
56.00	0.37	-0.05	0	0

TABLE 3.7
Live Load Effects (Shear)–SU7

	SAP2000		AASHTOWare BrR	
Station	**- V2**	**+ V2**	**-V2**	**+V2**
ft	**Kip-ft**	**Kip-ft**	**Kip-ft**	**Kip-ft**
0.00	-6.44	46.84	-6.69	45.24
5.60	-7.59	39.53	-6.69	37.88
11.20	-8.32	32.51	-6.69	30.83
16.80	-9.3	25.9	-8.54	24.2
22.40	-19.18	20.29	-14.61	18.08
28.00	-27.95	15.43	-21.09	12.62
33.60	-34.82	11.27	-28.467	7.84
39.20	-42.84	7.88	-36.28	3.64
44.80	-49.53	4.25	-43.84	1.67
50.40	-58.1	2.16	-51.32	1.708
56.00	-62.27	1.59	-58.05	1.74
0.00	-1.74	65.27	-1.59	58.05
7.10	-5.85	52.01	-5.47	46.87
14.20	-5.52	45.17	-5.47	40.03
21.30	-7.39	37.99	-6.41	32.82
28.40	-13.36	30.76	-12.07	25.55
35.50	-20.98	23.98	-18.65	18.66
42.60	-31.51	18.81	-26.19	12.371
49.70	-37.91	14.07	-34.47	6.74
56.80	-45.42	10.21	-42.94	5.87
63.90	-54.03	6.42	-51.447	5.99
71.00	-63.26	5.80	-59.54	6.13
0.00	-5.8	65.26	-6.13	59.54
5.60	-1.99	53.3	-1.56	47.06
11.20	-3.98	47.36	-1.56	41.16
16.80	-7.52	40.9	-3.5	34.71
22.40	-11.02	34.04	-7.66	27.81
28.00	-15.43	27.95	-12.62	21.09
33.60	-20.76	22.69	-18.508	14.956
39.20	-27.13	18.12	-25.35	8.94
44.80	-34.8	12.08	-33.01	7.16
50.40	-43.22	8.28	-41.446	7.314
56.00	-52.37	7.2	-50.58	7.47

smaller section to compute the section capacity. The rating factors were also computed using Mathcad from the member capacities and the dead and live loading.

These worksheets included a detailed calculation of the section properties, capacities, and rating factors of the member. The calculations for the bridge in question are shown below.

Length of span: L=71 ft.
Larger width of top flange: b_{tf1}=11.51 in.
Smaller width of top flange: b_{tf2}=11.48 in.
Larger thickness of top flange: t_{tf1}=0.855 in.
Smaller thickness of top flange: t_{tf2}=0.74 in.
Larger width bottom flange: b_{bf1}=11.51 in.
Smaller width of bottom flange: b_{bf2}=11.48 in.
Larger thickness of bottom flange: t_{bf1}=0.855 in.
Smaller thickness of bottom flange: t_{bf2}=0.74 in.
Larger depth of web: d_{w1}=31.38 in.
Smaller depth of web: d_{w2}=31.42 in.
Larger thickness of web: t_{w1}=0.58 in.
Smaller thickness of web: t_{w2}=0.55 in.

Total depth of larger girder: $d_1=d_{w1}+t_{tf1}+t_{bf1}$= 33.09 in.
Total depth of smaller girder: $d_2=d_{w2}+t_{tf2}+t_{bf2}$= 32.9 in.
Girder spacing: S=7.25 ft.
Deck thickness: t_{deck}=9 in.
Thickness of the sacrificial wearing surface: $t_{sacrificial}$ =0.5 in.
Effective thickness of deck: $t_{effective\ deck}=t_{deck}-t_{sacrificial}$=8.5 in.
Elastic modulus of steel: E_s=29,000 ksi
Compressive strength of steel: F_{yc}=50 ksi
Tensile strength of steel: F_{yt}=50 ksi
Yield strength of steel: F_y=50 ksi
Unbraced length: L_b=26.0225 ft.
Areas of cross section of bottom flange: $A_1=b_{bf2}*t_{bf2}$=8.495 in.^{2}
Centroid of bottom flange: $y_1=\frac{t_{bf2}}{2}$=0.37 in.
Areas of cross section of top flange: $A_2=b_{tf2}*t_{tf2}$=8.495 in.^{2}

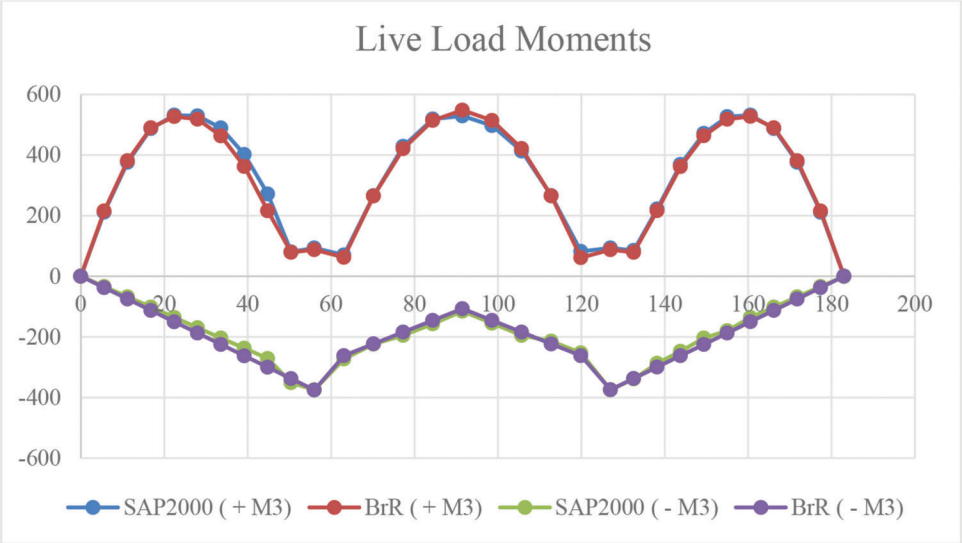

Figure 3.9 Comparison of live load moments.

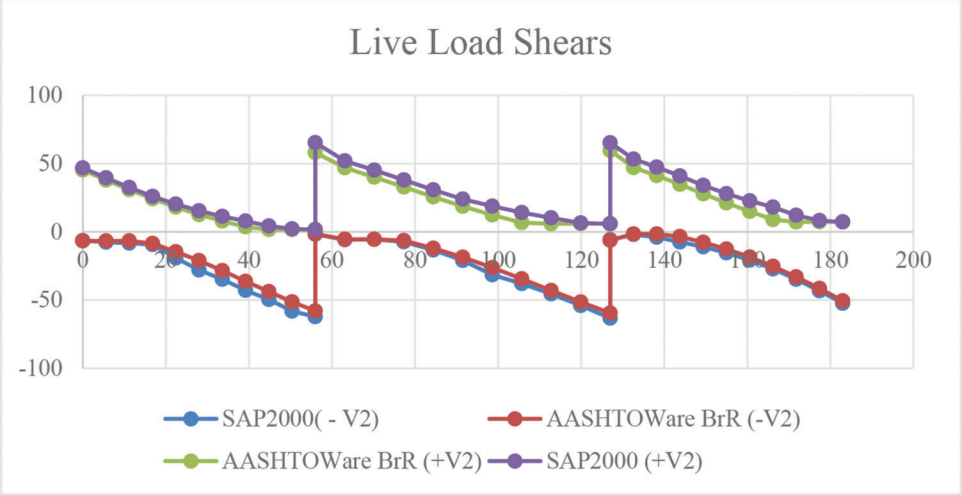

Figure 3.10 Comparison of live load shears.

Centroid of top flange: $y_2 = d_2 - \frac{t_{tf2}}{2} = 32.53$ in.

Area of cross section of web: $A_3 = d_{w2} * t_{w2} = 17.281$ in.^{2}

Centroid of web: $y_3 = d_2 - t_{tf2} - \frac{d_{w2}}{2} = 16.45$ in.

Position of the elastic neutral axis (ENA) from the bottom flange:

$$y_{ENA} = \frac{A_1 * y_1 + A_2 * y_2 + A_3 * y_3}{A_1 + A_2 + A_3} = 16.45 \text{ in.}$$

Therefore, the depth of the web in compression, D_c is given as

$$D_c = 2 * \frac{y_{ENA} - t_{bf2}}{2} = 15.71 \text{ in.}$$

Thus, the value of L_p and r_t are calculated using Equations 3.15 and 3.18, respectively,

$$L_p = 1.0 * 2.864 * \sqrt{\frac{29{,}000}{50}} = 68.971 \text{ in.} = 5.748 \text{ ft.}$$

$$r_t = \frac{11.48}{\sqrt{12 + \left(1 + \frac{1}{3} * \frac{15.71 * 0.55}{11.48 * 0.74}\right)}} = 2.864 \text{ in.}$$

For rolled shapes and homogenous built-up sections, $R_h = 1.0$

Calculation of F_{yr}:F_{yr} is the minimum of the values shown below:

1. $F_{yr1} = 0.7 * F_{yc} = 0.7 * 50$ ksi $= 35$ ksi
2. F_{yw}: for sections with $R_h = 1.0$, $F_{yw} = F_{yc} = 50$ ksi

Additionally,

should not be less than 0.5* F_{yc}=25 ksi. Therefore, F_{yr}=35 ksi.

L_r is calculated using Equation 3.16 as,

$$L_r = *2.864*\sqrt{\frac{29{,}000}{35}} = 258.982\,\text{in.} = 21.582\,\text{ft.}$$

Calculation of the web load shedding factor (R_b) is according to AASHTO 6.10.1.10.2

If the web satisfies $2*\frac{D_c}{t_{w1}} \le \lambda_{rw}$, then R_b=1.

Calculating $2*\frac{D_c}{t_{w1}}$,

$$2*\frac{15.71}{0.55} = 57.127$$

The value of λ_{rw} is defined as follows,

$$4.6*\sqrt{\frac{E_s}{F_{yc}}} \le \lambda_{rw} \le 5.7*\sqrt{\frac{E_s}{F_{yc}}}\ \text{(AASHTO 6.10.1.10.2-5)}$$

$$\lambda_{rw} = \left(3.1 + \frac{5.0}{a_{wc}}\right)*\sqrt{\frac{E_s}{F_{yc}}}$$

Where a_{wc} is equal to $2*D_c*\frac{t_{w2}}{b_{bf2}*t_{bf2}} = 2.034$

Therefore, $\lambda_{rw} = (3.1 + \frac{5}{2.034})*\sqrt{\frac{29{,}000}{50}} = 133.853$

$$4.6*\sqrt{\frac{E_s}{F_{yc}}} = 110.783$$

$$5.7*\sqrt{\frac{E_s}{F_{yc}}} = 137.274$$

Since λ_{rw} lies between 110.783 and 137.274, the value of λ_{rw} is 133.853.

Now, $2*\frac{D_c}{t_{w1}} = 57.127 < \lambda_{rw}$ (=133.853) (AASHTO 6.10.1.10.2-1)

therefore, R_b=1.0.

Since the member is non-prismatic within the unbraced length, AASHTO LRFD assumes the moment gradient modifier, C_b to be equal to 1.0. Although this is a conservative approach, the calculation proceeds by taking C_b=1 for comparison with BrR results.

Therefore, by Equation 3.17,

$$F_{cr} = \frac{1.0*\pi^2*29{,}000}{\left(\frac{26.0225}{2.864}\right)^2} = 24.074\,\text{ksi}$$

Calculating the lateral torsional buckling capacity, as L_b=26.0225 ft., L_p=5.748 ft. and L_r=21.582 ft., $L_b > L_r$. Therefore, Equation 3.14 is used to calculate lateral torsional buckling capacity, F_{nc}.

$F_{nc} = F_{cr} \le R_b R_h F_{yc}$.

$F_{nc} = F_{cr}$=24.074 ksi.

F_{nc} cannot exceed $R_b R_h F_{yc}$=1.0 * 1.0 * 50=50 ksi.

Hence, the lateral torsional buckling capacity of this member is computed to be equal to 24.074 ksi.

At this stage, comparisons with AASHTOWare BrR are made to check the capacity calculation therein. Screenshots of the AASHTOWare BrR reports are shown for comparisons.

It can be seen in Figure 3.11 that the lateral torsional buckling capacity calculated by BrR matches with the capacity computed separately using SAP2000 analysis. This implies that the capacity calculations are consistent with the provisions of the *AASHTO LRFD Design Manual* and are computed correctly.

Using the capacities and the analysis results from SAP2000, the rating factors are calculated. The calculations for the rating factor are carried out according to the provisions of the MBE (AASHTO, 2018).

The applied moment due to dead loads from Table 3.3 is,

Limit State	Load Comb	Flexure Type	Component	Dc (in)	rt	Fyc (ksi)	Lp (in)	Compact
STR-I	1, LegalS~	Pos**	Top Flange	---	---	---	---	---
STR-I	1, LegalS~	Neg	Bot Flange	15.690	2.864	50.0	69.0	No***
SER-II	1, LegalS~	Pos**	Top Flange	---	---	---	---	---
SER-II	1, LegalS~	Neg	Bot Flange	15.690	2.864	50.0	69.0	No***

Fyr (ksi)	Lr (in)	Slender	Cb	Mult	Fcr (ksi)	Rb	Rh	Fnc(LTB) (ksi)
---	---	---	---	---	---	---	---	---
35.0	259.0	Yes	1.000	---	24.1	1.000	1.000	24.08
---	---	---	---	---	---	---	---	---
35.0	259.0	Yes	1.000	---	24.1	1.000	1.000	24.08

Figure 3.11 LTB capacity–AASHTOWare BrR (AASHTO, 2021).

Component: Bot Flange

Load	Load Combo	Limit State	Flexure Type	LL (kip-ft)	Adj. LL (kip-ft)	DC	DW	DW-WS	LL
LegalSpecial	1	STR-I	neg	87.7	---	1.25	1.50	1.50	1.30
LegalSpecial	1	STR-I	neg	-374.8	---	1.25	1.50	1.50	1.30

Legend:
NA - Resistance and live load are of opposite sign so rating factor is not applicable.

fLLz (ksi)	fl (ksi)	Adj. fLLz (ksi)	Phi	fR (ksi)	---- Override ---- Phi	fR (ksi)	RF	Capacity (Ton)
2.59	0.00	---	1.00	-24.08	---	---	NA	NA
-11.09	0.00	---	1.00	-24.08	---	---	0.892	34.55

Figure 3.12 Rating factor–AASHTOWare BrR (AASHTO, 2021).

$$M_{DC} = 294.38 \text{ kip} - \text{ft}$$

The applied live load moment due to SU7 truck from Table 3.6 is,

$$M'_{LL} = 461.21 \text{ kip} - \text{ft}$$

Impact factor of 1.33 (33%) and distribution factor for this girder are applied. Therefore,

$$M_{LL} = M_{LL} * 1.33 * 0.611 = 374.79 \text{ kip} - \text{ft}$$

The stresses are calculated using these moments and the computed section moduli.

$$f_{DC} = \frac{M_{DC}}{S_x} = 8.71 \text{ ksi} \quad f_{LL} = \frac{M_{LL}}{S_x} = 11.09 \text{ ksi}$$

Here S_x is the section modulus (in.^{3}) and is equal to 405.56 in.^{3}

Using these values of stresses and capacity, the rating factor is calculated.

$$RF = \frac{F_{nc} - (\gamma_{DC} * f_{DC})}{(\gamma_L * f_{LL})} = \frac{24.074 - (1.25 * 8.71)}{(1.3 * 11.09)} = 0.915$$

Here, $\gamma_{DC} = 1.25$ and $\gamma_L = 1.3$.

The rating factor calculated in AASHTOWare BrR is shown in Figure 3.12. For lateral torsional buckling capacity, the compression flange capacity is checked. The point where the rating factor is checked lies in the negative flexure region. Thus, the compression flange is the bottom flange.

It can be observed that the rating factor calculated by separate analysis and computation is slightly different from the calculated value in the AASHTOWare software. The difference between the two values is 0.915–0.892 = 0.023. The minor differences between the dead load and live load moments as seen in Table 3.3 and Table 3.6 respectively, can be held accountable for this difference in the rating factors. Moreover, both rating factor (RF) values, as they are presently determined, are less than 1.0, which means that lateral torsional buckling capacity for the bridge is not adequate. The condition could be rectified by adding a brace to increase the lateral torsional buckling strength, or by posting the bridge to control the loading permitted.

It can be seen through these results that AASHTOWare software follows the provisions of the *LRFD Bridge Design Specifications* (AASHTO, 2020). Although the software is consistent with the specifications, there are some observations that were drawn while examining the BrR results. The next section discusses these observations and some recommendations that can be made to improve the accuracy of results.

3.3 Discussion

This section examines some of the observations made from AASHTOWare BrR results and from the calculations performed in the previous section. Careful examination of the results and further reading about lateral torsional buckling leads to a discussion about some changes that can be incorporated.

3.3.1 Changes in Cross Section

3.3.1.1 Moment gradient. The moment gradient modifier, C_b is a factor which corresponds to the increase in critical moment capacity, compared to an unbraced beam segment subjected to uniform moment, as a result of the variation in the moment along the length between the two brace points. The value of C_b is taken as equal to 1.0 when the moment does not vary within the unbraced length of the member. In other words, a value of C_b equal to 1.0 is the worst-case scenario or the most conservative case. The calculation of C_b, as noted in Section 3.1.3, is limited to the members in which the unbraced length is prismatic. Section 6.10.8.2.3 in the *LRFD Bridge Design Specifications* (AASHTO, 2020) require that C_b

should be taken equal to 1.0 if the member is non-prismatic within the unbraced length.

Moreover, it was observed that there was a significant variation of the moment within the unbraced lengths of the bridges examined for this research for which a section changes occur. The use of $C_b = 1$ for many of these bridges is very conservative and certainly not "correct."

Previous research studies have shown that the moment gradient modifier can be computed using a different approach for stepped beams (Park & Kang, 2004; Park & Stalling, 2003, 2005). Stepped beams are the sections where the cross section is changed suddenly, usually increased near the piers to resist large negative moments. A stepped beam within an unbraced segment is a non-prismatic section. A set of equations is suggested by Park and Stallings (2003) for the C_b calculation. The research compares the results from the proposed equations with FEM models to bolster its validity for various stepped beam scenarios.

Under general loading conditions, the proposed design equation for stepped beams is given as,

$$M_{st} = C_{bst} C_{st} M_{ocr} \qquad \text{(Equation 3.23)}$$

where,

$$C_{st} = C_o + 6\alpha^2\left(\beta\gamma^{1.3} - 1\right) \text{ (doubly} - \text{stepped beams)} \qquad \text{(Equation 3.24)}$$

$$C_{st} = C_o + 1.5\alpha^{1.6}\left(\beta\gamma^{1.2} - 1\right) \text{ (singly} - \text{stepped beams)} \qquad \text{(Equation 3.25)}$$

C_o is a constant depending on the number of inflection points in the deflected shape within unbraced length. The variables α, β, and γ are the ratios as defined in Figure 3.13.

M_{ocr} is the LTB moment of an equal length prismatic beam having the smaller cross section along the entire span.

For cases with no inflection points, C_o should be taken as one. For the calculation of C_{bst},

$$C_{bst} = \frac{12.5M_{max}}{2.5M_{max} + 3M_A + 4M_B + 3M_C} \qquad \text{(Equation 3.26)}$$

Equation 3.26 is the equation as used in the *Specification for Structural Steel Buildings* (AISC, 2016). Here, M_{max} is the maximum moment within the unbraced length, M_A, M_B and M_C are the fourth point moments, i.e., at 1/4, 1/2, and 3/4 length of the unbraced length.

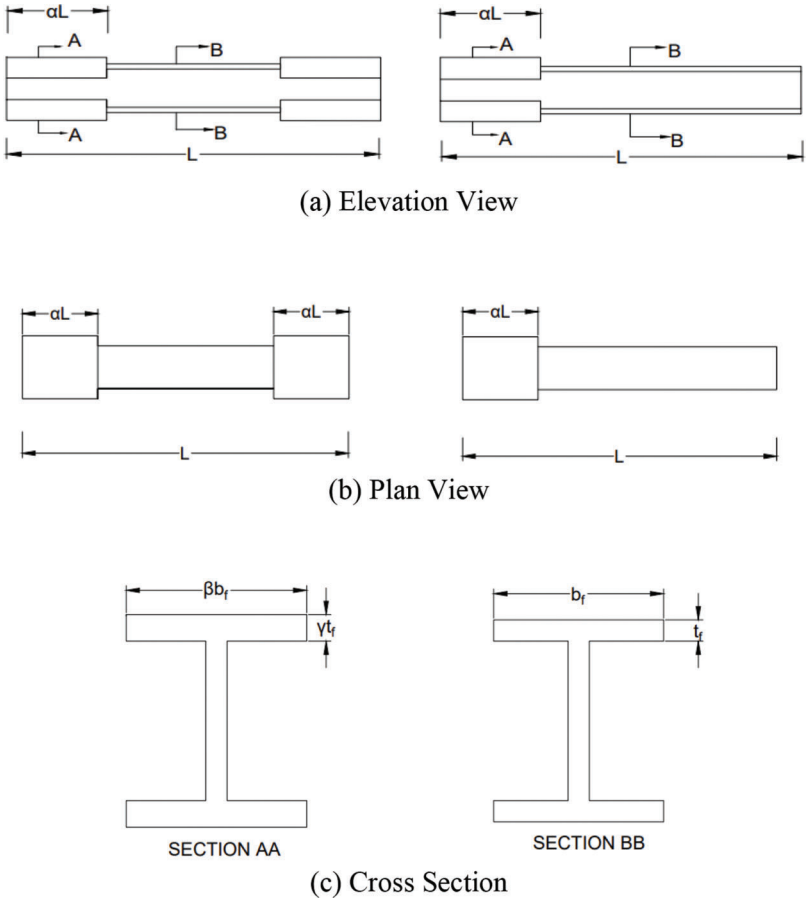

Figure 3.13 Parameters for doubly and singly stepped beams (Park & Stallings, 2003).

For cases with one inflection point within the unbraced length, C_o should be taken as 1. C_{bst} is calculated as,

$$C_{bst} = \frac{10M_{max}}{4M_{max} + M_A + 7M_B + M_C} \quad \text{(Equation 3.27)}$$

For cases with two inflection points, or two zero moment points, C_o should be taken as 0.85. C_{bst} is computed using Equation 3.27.

3.3.1.1.1 Example for C_b *calculation for a non-prismatic section.* The structure considered for this example is the same as considered in Section 3.2. The moment gradient factor was taken equal to 1.0 previously. In the present example, a new C_b is calculated using the approach provided by Park and Stallings (2003). The unbraced length for the girder was L_b = 26.0225 ft.

The section is non-prismatic within the unbraced length and the elevation view of the girder is shown in Figure 3.14.

1. Determine the number inflection points within the unbraced length. From the moment diagram in SAP2000 and Table 3.3, it can be seen that there is one inflection point within the unbraced length. Therefore,

$$C_{bst} = \frac{10M_{max}}{4M_{max} + M_A + 7M_B + M_C}$$

from Table 3.3 and 3.6,

$$M_{max} = 294.39 + 374.79 = 669.18 \text{ kip} - \text{ft}$$

$$M_A = 145.24 + 271.28 = 416.52 \text{ kip} - \text{ft}$$

$$M_B = 26.0069 + 229.42 = 255.427 \text{ kip} - \text{ft}$$

$$M_C = 62.7 + 193.85 = 256.55 \text{ kip} - \text{ft}$$

The values of M_A, M_B, and M_C are determined by interpolation at each quarter point.

$$C_{bst} = \frac{10(669.18)}{4(669.18) + (416.52) + 7(255.427) + (256.55)} = 1.302$$

2. Next step is to find C_{st}. As there is a singly stepped beam here, we use the equation

$$C_{st} = C_o + 1.5\ \alpha^{1.6}\ (\beta\gamma^{1.2} - 1)$$

$$\alpha = \frac{15.25}{26.0225} = 0.586\ \beta = \frac{11.51}{11.48} = 1.0026, \gamma = \frac{0.855}{0.74} = 1.155$$

C_o = 1, as there is one inflection points within the unbraced length.
Therefore,

$$C_{st} = 1 + 1.5 * (0.586)^{1.6}\left(1.0026 * (1.155)^{1.2} - 1\right) = 1.122$$

Thus,

$$C_b = C_{bst} C_{st} = 1.461$$

3. Using the new C_b, the modified capacity is,

$$C = F_{nc} = C_b * \left(1 - \left(1 - \frac{F_{yr}}{R_h * F_{yc}}\right) * \left(\frac{L_b - L_p}{L_r - L_p}\right)\right.$$

$$* R_b * R_h * F_{yc} = 1.461 * 24.074 = 35.18 \text{ ksi}$$

4. Using this modified capacity, the new rating factor is calculated. Using the calculated values of f_{DC} and f_{LL} as seen in Section 3.2,

$$RF = \frac{C - (\gamma_{DC} * f_{DC}) + (\gamma_p * P)}{\gamma_L * f_{LL}} = 1.685$$

Here,

$$\gamma_{DC} = 1.25,\ \gamma_p = 1.0,\ \gamma_L = 1.3$$

$$f_{DC} = 8.71,\ ksi\ P = 0,\ f_{LL} = 11.09 \text{ ksi}$$

The stepped beam C_b approach was used to calculate the moment gradient factor for non-prismatic sections; these are hereafter labeled as NP to indicate use of C_b to account for the non-prismatic section. Out of the 14 bridge files sent for examination by INDOT, 7 of them utilized C_b = 1.0 due to non-prismatic sections within the unbraced length. These analyses done with the default C_b value of 1.0, and they are labeled as DF to indicate that the default C_b value was used. These structures with their stepped beam C_b and modified rating factors are listed in Table 3.8.

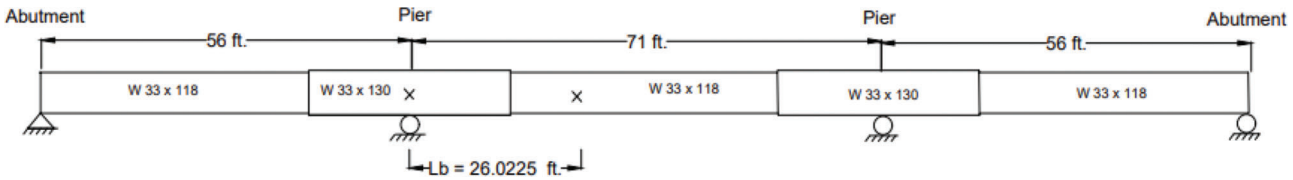

Figure 3.14 Non-prismatic girder–unbraced length.

The results shown in Table 3.8 correspond to the vehicles that were the most critical for these bridges. As can be observed the most critical vehicle is satisfied for all bridges, along with all the other rating vehicles, i.e., they produce a rating factor of more than one.

Another research study by Reichenbach et al. (2020) was conducted to calculate the C_b for girders with stepped flanges. This research was conducted along with the subcommittee of AASHTO T14 (Steel Bridge Committee). The proposed C_b by this research is same as Equation 3.26 multiplied by R_m where R_m is 1.0 for single curvature bending and $0.5+2\left(\frac{I_{ytop}}{I_y}\right)^2$ for reverse curvature bending. I_{ytop} is the moment of inertia of the top flange and I_y is the moment of inertia of the entire section. This is a recent study and although for this research the approach discussed earlier (Park & Stallings, 2003) is used, C_b is also computed using the latest study (Reichenbach et al., 2020). Table 3.9 compares C_b by both the approaches.

It can be noticed that C_b for both approaches provides a value that exceeds 1.0.

3.3.1.2 Tapered cover plate. Cover plates which have a linear change in width are called as tapered cover plates. The geometry of a tapered cover plate is illustrated in Figure 3.15.

In Figure 3.15, B1 and B2 are the widths of the cover plate. The width increases from B1 to B2 over a length of L1. The cover plate width remains constant for a length of L2.

Tapered cover plates were observed in some of the structures reviewed for this research. One such structure was I70-008-02344 BWBL. The cover plate width B1 was 3 in. and B2 was 13 in. L1 was 2 ft. and L2 was 14 ft. This cover plate is attached to the top and bottom flanges of a W30 × 116 I-shape. For calculating the effective width at the point where the width is B1, AASHTOWare BrR uses the expression,

$$\frac{(b_{fc} * t_f)+(B1 * T)}{(t_f+T)} \qquad \text{(Equation 3.28)}$$

Here, b_{fc} is the width of the flange of the beam, t_f is the thickness of flange and T is the thickness of the cover plate.

The value of this effective width is used for the calculation of the radius of gyration, r_t. As the I-shape is W30 × 116, b_{fc} is 10.495 in., t_f is 0.85 in., and the thickness T of the cover plate is 0.875 in. Using Equation 3.28, the effective width equals to 6.69 in.

TABLE 3.8
Modified Capacities and Rating Factors

Structure No.	Critical Vehicle	α	New NP C_b	Capacity (ksi)		Rating Factor	
				DF	NP	DF	NP
049-64-06679 CNBL	NRL	0.181	1.177	30.56	35.97	0.712	1.014
049-64-06679 CSBL	NRL	0.181	1.177	30.56	35.97	0.712	1.014
912-45-06599	EV3 Lane	0.722	1.553	26.64	41.37	0.927	1.893
234-83-07152	EV3 Lane	0.453	2.300	37.72	50.00	0.855	1.549
025-09-06941	Lane-Type Legal Load	0.448	2.170	29.45	50.00	0.628	2.233
I70-079-02420 E	HS20 (Lane Type)	0.765	2.140	27.83	50.00	0.490	2.188

TABLE 3.9
C_b Comparison

Structure No.	C_b (Park & Stalling, 2003)	C_b (Reichenbach et al., 2020)
049-64-06679 CNBL	1.177	1.403
049-64-06679 CSBL	1.177	1.403
912-45-06599	1.553	2.091
234-83-07152	2.300	1.346
025-09-06941	2.170	1.717
I70-079-02420 E	2.140	1.885
009-30-06644	1.461	1.403

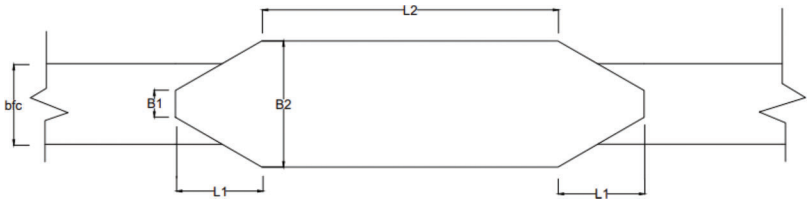

Figure 3.15 Tapered cover plate.

This leads to reduced capacity from one side. The capacity at the same location for the other side where the cover plate does not exist, is "adequate" as the effective width for r_t calculation was 10.495 in. for the W30 × 116, but the reduced effective width of 6.6932 in. is used at the point where the cover plate begins. The cover plate provides an extra inertia to the flange which itself is adequate for the loads at that location. That is why adding an extra cover plate should not reduce the lateral torsional buckling capacity in the tapered region of the cover plate.

AASHTOWare BrR assumes the smallest value of capacity produced due to a low r_t, throughout the unbraced length, therefore generating an extremely low rating factor. This assumption is certainly not accurate since the lateral torsional buckling capacity is not based on the capacity at a particular point, but the entire unbraced length. AASHTOWare BrR assumes the LTB capacity as the smallest capacity produced at a point within the unbraced length.

To resolve this issue, a new approach is suggested. The effective width of the cover plate, b_{eff}, is calculated through the new approach and the same effective width is used throughout the length of the cover plate. The new effective width is calculated by using the logic of proportions. The expression proposed to be used is,

$$b_{eff} = \left\{\frac{(B1+B2)}{2} * \frac{L1}{2L1+L2}\right\} + \left\{B2 * \frac{L2}{2L1+L2}\right\} + \left\{\frac{(B1+B2)}{2} * \frac{L1}{2L1+L2}\right\} \quad \text{(Equation 3.29)}$$

The equation is based on the idea that the width is multiplied by the fraction of the length for which it exists. For the tapered portion, it is suggested to be conservative and take the average width of the cover plate over the fraction of the tapered length to the overall length. By using this method, a single value of effective width is assumed throughout the length of the plate, and it is modeled like a rectangular plate. The effective width by this expression is,

$$\left\{\frac{(13in+3in)}{2} * \frac{2ft}{2*2ft+14ft}\right\} + \left\{13in * \frac{14ft}{2*2ft+14ft}\right\} + \left\{\frac{(13in+3in)}{2} * \frac{2ft}{2*2ft+14ft}\right\}$$

This produces a value of 11.88 in. Now, the cover plate is assumed to be a rectangular plate with the width of 11.88 in. throughout the overall length of 18 ft. The thickness of the cover plate is considered constant throughout the length and is equal to 0.875 in. in this case. The effective thickness thus, is the sum of the thickness of the W30 × 116 flange (0.85 in.) and the thickness of the cover plate (0.875 in.). Therefore, the total thickness is 0.875 + 0.85 = 1.725 in. This ensures that there is enough capacity throughout the unbraced length from both sides of the cover plate end.

This approach provides an approximate method to handle girders with tapered cover plates. It is important to notice that the effective width of the cover plate by Equation 3.29 (11.88 in.) gives a value lesser than the width B2 (13 in.). This approach can be a way to modify a tapered cover plate by modelling it as a rectangular cover plate to avoid sudden capacity drops in the tapered region.

3.3.2 AASHTOWare BrR

The two approaches discussed in the previous section, namely moment gradient factor for non-prismatic sections and tapered cover plates, can be incorporated into AASHTOWare BrR for practical use.

3.3.2.1 Moment gradient–capacity override. The modified moment gradient factor calculated for non-prismatic sections can be assimilated into AASHTOW are BrR software by using the feature of capacity override. Table 3.8 lists the new capacities after the modified moment gradient factors have been applied. The following screenshots from AASHTOWare BrR show how these capacities can be inputted. For this example, the structure No. 234-83-07152 is analyzed. The modified capacity, as seen in Table 3.8, is 50 ksi for this structure.

Figure 3.16 shows the points of interest at the location where the new capacity is defined. The user can manually input the points of interest to modify the capacity at that location.

Figure 3.17 illustrates the screen where the new compression capacity calculated using the stepped beam C_b and phi factor can be inputted manually. No other limit states were noted to occur after the change was made at the POI.

Figure 3.18 shows the rating factor calculated in AASHTOWare BrR using the capacity computed using the default value of $C_b = 1$. It can be seen that the value of the rating factor is 0.855 for EV3 (Lane - Type) loading for "Legal pair + lane."

Figure 3.19 shows the newly calculated rating factor using the new capacity that was inputted as shown in Figure 3.17.

It is apparent that the new rating factor of 1.549 is calculated for the over-ridden capacity of 50 ksi for the increased C_b factor for the non-prismatic section.

3.3.2.2 Tapered cover plates–modeling. The revised effective width of tapered cover plate for the structure I70-008-02344 BWBL, as computed using Equation 3.29, can be used practically in BrR as shown in the following screenshots.

Figure 3.20 shows the widths of the top tapered cover plates, before modification, with the length variations that exist.

The new effective widths of the top tapered cover plates that are calculated using Equation 3.29, can be inputted as shown in Figure 3.21. There are three cover plates here with the calculated effective widths as 11.88 in., 12.024 in., and 11.88 in. As noted

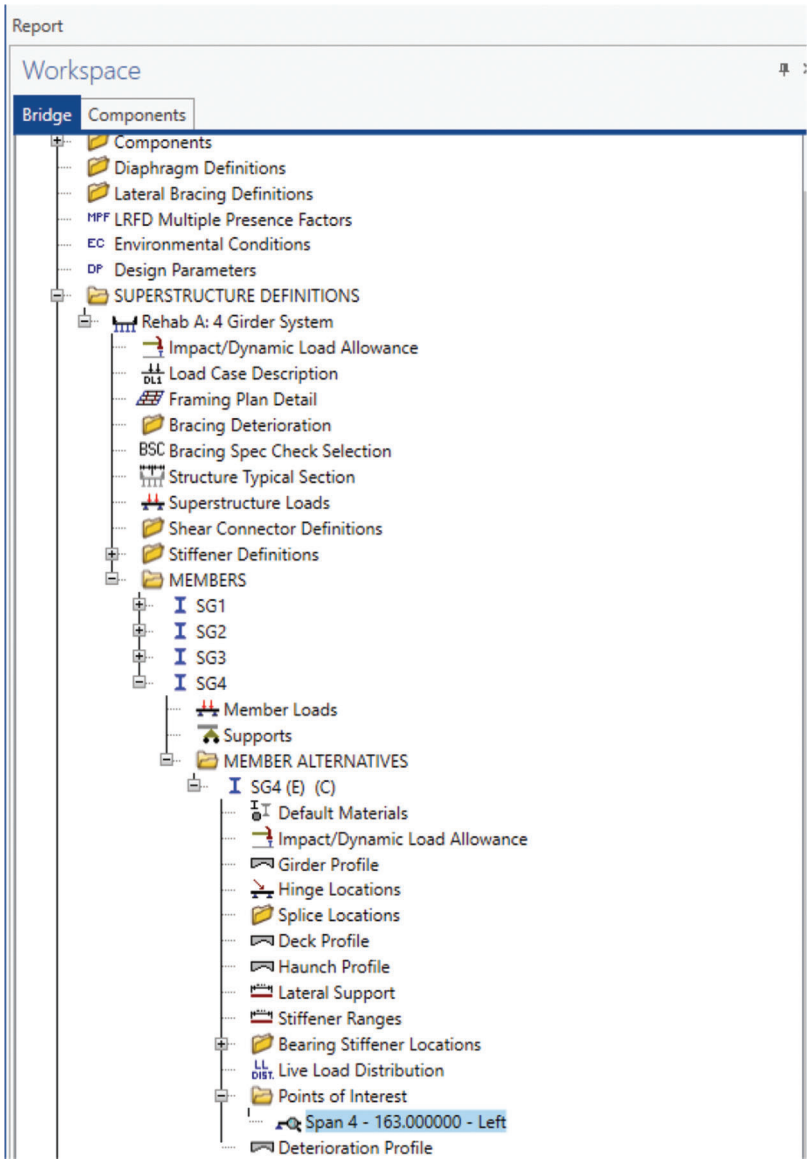

Figure 3.16 Points of interest (AASHTO, 2021).

before, the effective width is appropriate with a fixed dimension since the lateral torsional strength corresponds to the strength over a given unbraced length and does not change at locations within that unbraced length.

Figure 3.22 shows the widths of the bottom tapered cover plates that are used in BrR to conduct the calculations, before modification.

The effective widths for the bottom tapered cover plates are calculated using Equation 3.29 and are inputted in BrR as shown in Figure 3.23. There are seven cover plates here with the calculated effective widths as 8.85 in., 11.88 in., 9.023 in., 12.024 in., 9.023 in., 11.88 in., and 8.85 in.

After the cover plate is modeled as shown, the analysis is run again and the comparisons between the old and modified rating factors are shown in Figures 3.24 and 3.25, respectively.

The rating factor increases from 0.758 to 3.182 by modeling the cover plate using Equation 3.29.

3.3.3 AASHTOWare BrR

Sections 3.3.1 and 3.3.2 discuss some modifications that can be considered for cases like changes in cross section (stepped beam) or tapered covered plates. Out of the 14 bridge files sent by INDOT, these recommendations were valid for 8 structures, 7 for changes in cross section by using stepped beam C_b, and 1 for tapered covered plate. The problems with the remaining 6 bridges are discussed in this section.

There was one bridge, P000-47-07089 which had no diaphragms or cross frames providing bracing between the supports. It is a short, three-span bridge with span lengths as 11.5 ft., 16.0833 ft., and 11.5 ft. The bridge

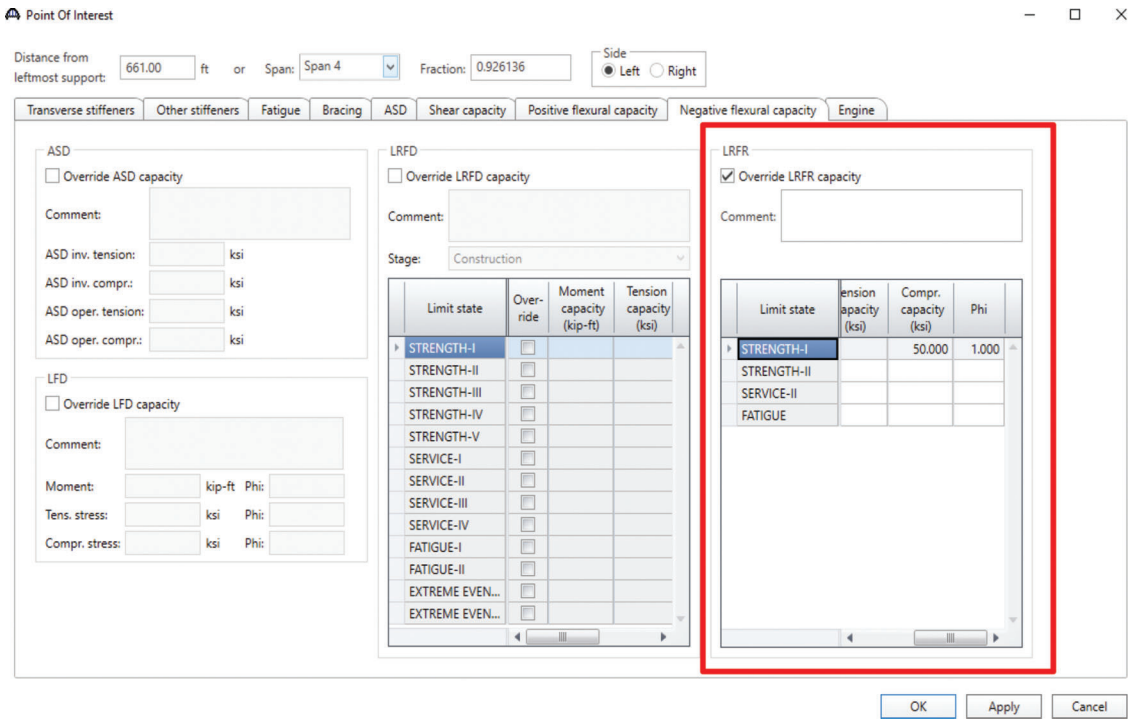

Figure 3.17 Capacity override–negative flexure (AASHTO, 2021).

Component: Bot Flange

Load	Load Combo	Limit State	Flexure Type	LL (kip-ft)	Adj. LL (kip-ft)	DC	DW	DW-WS	LL
LegalRoutine	1	STR-I	neg	0.0	---	1.25	1.50	1.50	1.30
LegalRoutine	1	STR-I	neg	0.0	---	1.25	1.50	1.50	1.30
LegalRoutine	2	STR-I	neg	0.0	---	1.25	1.50	1.50	1.30
LegalRoutine	2	STR-I	neg	-2213.8	---	1.25	1.50	1.50	1.30

Load Combination Legend:

Code	Vehicle
1	EV3 - Indiana (Lane -Type) - Legal Truck + Lane
2	EV3 - Indiana (Lane -Type) - Legal Pair + Lane

fLLz (ksi)	fl (ksi)	Adj. fLLz (ksi)	Phi	fR (ksi)	---- Override ---- Phi	fR (ksi)	RF	Capacity (Ton)
0.00	0.00	---	1.00	-37.72	---	---	99.000	3192.75
0.00	0.00	---	1.00	-37.72	---	---	99.000	3192.75
0.00	0.00	---	1.00	-37.72	---	---	99.000	6385.50
-13.63	0.00	---	1.00	-37.72	---	---	0.855	55.16

Figure 3.18 Rating factor with default $C_b = 1$ value (AASHTO, 2021).

fails in the second span and the unbraced length was the entire span length of 16.0833 ft.

Structure No. I70-123-02361 JDEB, passed for all the legal loads except for EV3 lane type legal load for the combination of "truck pair + lane." The lateral torsional buckling capacity of this bridge was pushed to maximum, i.e., 36 ksi as A-36 steel was used for the girders. Although the capacity was maximum, it was still not adequate to bear the load effects of the EV3 lane type legal load, which were extremely high.

Component: Bot Flange

Load	Load Combo	Limit State	Flexure Type	LL (kip-ft)	Adj. LL (kip-ft)	DC	DW	DW-WS	LL
LegalRoutine	1	STR-I	neg	0.0	---	1.25	1.50	1.50	1.30
LegalRoutine	1	STR-I	neg	0.0	---	1.25	1.50	1.50	1.30
LegalRoutine	2	STR-I	neg	0.0	---	1.25	1.50	1.50	1.30
LegalRoutine	2	STR-I	neg	-2213.8	---	1.25	1.50	1.50	1.30

Load Combination Legend:

Code	Vehicle
1	EV3 - Indiana (Lane -Type) - Legal Truck + Lane
2	EV3 - Indiana (Lane -Type) - Legal Pair + Lane

fLLz (ksi)	fl (ksi)	Adj. fLLz (ksi)	Phi	fR (ksi)	---- Override ---- Phi	fR (ksi)	RF	Capacity (Ton)
0.00	0.00	---	1.00	-50.00	1.00	-50.00	99.000	3192.75
0.00	0.00	---	1.00	-50.00	1.00	-50.00	99.000	3192.75
0.00	0.00	---	1.00	-50.00	1.00	-50.00	99.000	6385.50
-13.63	0.00	---	1.00	-50.00	1.00	-50.00	1.549	99.89

Figure 3.19 Rating factor for modified C_b value (AASHTO, 2021).

Girder Profile

Type: Rolled Shape

Shape | Top cover plate | Bottom cover plate

Welded Bolted

Relative position	Begin width (in)	End width (in)	Thickness (in)	Support number	Start distance (ft)	Length (ft)	End distance (ft)	Material	Side weld	End weld at right
1	3.0000	13.0000	0.8750	1	49.75	2.00	51.75	ASTM	-- Non	-- Non
1	13.0000	13.0000	0.8750	1	51.75	14.00	65.75	ASTM	-- Non	-- Non
1	13.0000	3.0000	0.8750	2	7.00	2.00	9.00	ASTM	-- Non	-- Non
1	3.0000	13.0000	0.8750	2	65.00	2.00	67.00	ASTM	-- Non	-- Non
1	13.0000	13.0000	0.8750	2	67.00	16.50	83.50	ASTM	-- Non	-- Non
1	13.0000	3.0000	0.8750	3	8.25	2.00	10.25	ASTM	-- Non	-- Non
1	3.0000	13.0000	0.8750	3	66.25	2.00	68.25	ASTM	-- Non	-- Non
1	13.0000	13.0000	0.8750	3	68.25	14.00	82.25	ASTM	-- Non	-- Non
1	13.0000	3.0000	0.8750	4	7.00	2.00	9.00	ASTM	-- Non	-- Non

Figure 3.20 Top cover plate–variable widths (AASHTO, 2021).

The structure I70-076-02376 B showed some unusual results. The structure consists of three spans and the bridge is inadequate in shear at 14 ft. into the third span as shown when rated by the LRFR methodology. There was a spike in shear observed at this location. This behavior is unusual because shear is generally a maximum at the member ends and decreases away from the ends. This abnormal increase in shear force led the rating factor being extremely low at that location. The location of the shear spike is shown in Figure 3.26.

The spike in the shear can be noted in Figure 3.27. It represents a screenshot of the report generated for LRFR analysis in AASHTOWare BrR for SU6 Truck using the feature "Report Tool."

Here, nodes 68 and 69 denote the location of 14 ft. into span 3 and there is a sudden jump observed from node 68 (-163.005 kips) to node 69 (-926.391 kips). The value of -926.391 kips is extremely high and such a high value at a location away from the ends of span is not justified. A separate analysis in SAP2000 was run to check the values produced by AASHTOWare BrR.

Girder Profile

Type: Rolled Shape

Shape | Top cover plate | Bottom cover plate

Welded / Bolted

Relative position	Begin width (in)	End width (in)	Thickness (in)	Support number	Start distance (ft)	Length (ft)	End distance (ft)	Material	Side weld	End weld at right
1	11.8800	11.8800	0.8750	1	49.75	2.00	51.75	ASTM	-- Non	-- Non
1	11.8800	11.8800	0.8750	1	51.75	14.00	65.75	ASTM	-- Non	-- Non
1	11.8800	11.8800	0.8750	2	7.00	2.00	9.00	ASTM	-- Non	-- Non
1	12.0240	12.0240	0.8750	2	65.00	2.00	67.00	ASTM	-- Non	-- Non
1	12.0240	12.0240	0.8750	2	67.00	16.50	83.50	ASTM	-- Non	-- Non
1	12.0240	12.0240	0.8750	3	8.25	2.00	10.25	ASTM	-- Non	-- Non
1	11.8800	11.8800	0.8750	3	66.25	2.00	68.25	ASTM	-- Non	-- Non
1	11.8800	11.8800	0.8750	3	68.25	14.00	82.25	ASTM	-- Non	-- Non
1	11.8800	11.8800	0.8750	4	7.00	2.00	9.00	ASTM	-- Non	-- Non

Figure 3.21 Top cover plate–fixed effective width. (AASHTO, 2021).

Girder Profile

Type: Rolled Shape

Shape | Top cover plate | Bottom cover plate

Welded / Bolted

Relative position	Begin width (in)	End width (in)	Thickness (in)	Support number	Start distance (ft)	Length (ft)	End distance (ft)	Material	Side weld	End weld at right
1	3.0000	9.5000	0.7500	1	13.83	2.00	15.83	ASTM	-- Non	-- Non
1	9.5000	9.5000	0.7500	1	15.83	16.00	31.83	ASTM	-- Non	-- Non
1	9.5000	3.0000	0.7500	1	31.83	2.00	33.83	ASTM	-- Non	-- Non
1	3.0000	13.0000	0.8750	1	49.75	2.00	51.75	ASTM	-- Non	-- Non
1	13.0000	13.0000	0.8750	1	51.75	14.00	65.75	ASTM	-- Non	-- Non
1	13.0000	3.0000	0.8750	2	7.00	2.00	9.00	ASTM	-- Non	-- Non
1	3.0000	9.5000	0.7500	2	24.00	2.00	26.00	ASTM	-- Non	-- Non
1	9.5000	9.5000	0.7500	2	26.00	23.25	49.25	ASTM	-- Non	-- Non
1	9.5000	3.0000	0.7500	2	49.25	2.00	51.25	ASTM	-- Non	-- Non
1	3.0000	13.0000	0.8750	2	65.00	2.00	67.00	ASTM	-- Non	-- Non
1	13.0000	13.0000	0.8750	2	67.00	16.50	83.50	ASTM	-- Non	-- Non
1	13.0000	3.0000	0.8750	3	8.25	2.00	10.25	ASTM	-- Non	-- Non
1	3.0000	9.5000	0.7500	3	24.00	2.00	26.00	ASTM	-- Non	-- Non
1	9.5000	9.5000	0.7500	3	26.00	23.25	49.25	ASTM	-- Non	-- Non
1	9.5000	3.0000	0.7500	3	49.25	2.00	51.25	ASTM	-- Non	-- Non
1	3.0000	13.0000	0.8750	3	66.25	2.00	68.25	ASTM	-- Non	-- Non
1	13.0000	13.0000	0.8750	3	68.25	14.00	82.25	ASTM	-- Non	-- Non
1	13.0000	3.0000	0.8750	4	7.00	2.00	9.00	ASTM	-- Non	-- Non
1	3.0000	9.5000	0.7500	4	24.92	2.00	26.92	ASTM	-- Non	-- Non
1	9.5000	9.5000	0.7500	4	26.92	16.00	42.92	ASTM	-- Non	-- Non
1	9.5000	3.0000	0.7500	4	42.92	2.00	44.92	ASTM	-- Non	-- Non

Figure 3.22 Bottom cover plate–variable width (AASHTO, 2021).

The method of influence lines was used to calculate the maximum value of shear produced by an SU6 Truck at 14 ft. into span 3 (see Figure 3.28). The calculated value was -165.16 kips. Thus, the shear of -163.005 kips can be justified, but the sudden spike cannot.

There were three bridges which rated more than 1.0 for all the AASHTO and Indiana legal loads. These bridges were 062-13-07329 A, I465-131-07719 A and I70-123-02361 DWBL. It is believed that these bridges must have undergone rehabilitation or an

Girder Profile

Type: Rolled Shape

Shape | Top cover plate | Bottom cover plate

Welded | Bolted

Relative position	Begin width (in)	End width (in)	Thickness (in)	Support number	Start distance (ft)	Length (ft)	End distance (ft)	Material	Side weld	End weld at right
1	8.8500	8.8500	0.7500	1	13.83	2.00	15.83	ASTM	-- Non	-- Non
1	8.8500	8.8500	0.7500	1	15.83	16.00	31.83	ASTM	-- Non	-- Non
1	8.8500	8.8500	0.7500	1	31.83	2.00	33.83	ASTM	-- Non	-- Non
1	11.8800	11.8800	0.8750	1	49.75	2.00	51.75	ASTM	-- Non	-- Non
1	11.8800	11.8800	0.8750	1	51.75	14.00	65.75	ASTM	-- Non	-- Non
1	11.8800	11.8800	0.8750	2	7.00	2.00	9.00	ASTM	-- Non	-- Non
1	9.0230	9.0230	0.7500	2	24.00	2.00	26.00	ASTM	-- Non	-- Non
1	9.0230	9.0230	0.7500	2	26.00	23.25	49.25	ASTM	-- Non	-- Non
1	9.0230	9.0230	0.7500	2	49.25	2.00	51.25	ASTM	-- Non	-- Non
1	12.0240	12.0240	0.8750	2	65.00	2.00	67.00	ASTM	-- Non	-- Non
1	12.0240	12.0240	0.8750	2	67.00	16.50	83.50	ASTM	-- Non	-- Non
1	12.0240	12.0240	0.8750	3	8.25	2.00	10.25	ASTM	-- Non	-- Non
1	9.0230	9.0230	0.7500	3	24.00	2.00	26.00	ASTM	-- Non	-- Non
1	9.0230	9.0230	0.7500	3	26.00	23.25	49.25	ASTM	-- Non	-- Non
1	9.0230	9.0230	0.7500	3	49.25	2.00	51.25	ASTM	-- Non	-- Non
1	11.8800	11.8800	0.8750	3	66.25	2.00	68.25	ASTM	-- Non	-- Non
1	11.8800	11.8800	0.8750	3	68.25	14.00	82.25	ASTM	-- Non	-- Non
1	11.8800	11.8800	0.8750	4	7.00	2.00	9.00	ASTM	-- Non	-- Non
1	8.8500	8.8500	0.7500	4	24.92	2.00	26.92	ASTM	-- Non	-- Non
1	8.8500	8.8500	0.7500	4	26.92	16.00	42.92	ASTM	-- Non	-- Non
1	8.8500	8.8500	0.7500	4	42.92	2.00	44.92	ASTM	-- Non	-- Non

Figure 3.23 Bottom cover plate–fixed effective width (AASHTO, 2021).

Component: Bot CP 1

Load	Load Combo	Limit State	Flexure Type	LL (kip-ft)	Adj. LL (kip-ft)	DC	DW	DW-WS	LL
LegalSpecial	1	STR-I	neg	135.4	---	1.25	1.50	1.50	1.45
LegalSpecial	1	STR-I	neg	-331.4	---	1.25	1.50	1.50	1.45

Legend:
NA - Resistance and live load are of opposite sign so rating factor is not applicable.

fLLz (ksi)	fl (ksi)	Adj. fLLz (ksi)	Phi	fR (ksi)	---- Override ---- Phi	fR (ksi)	RF	Capacity (Ton)
3.56	0.00	---	1.00	-36.00	---	---	NA	NA
-8.70	0.00	---	1.00	-16.21	---	---	0.758	30.33

Figure 3.24 Rating factor–based on variable width (AASHTO, 2021).

update within BrR which led to the rating factor being more than 1.0.

3.4 Recommendations

The previous sections discuss some modifications that can be implemented to achieve more accurate and less conservative results when using the LRFR methodology. This section presents the final recommendations that could be adopted by INDOT to continue using BrR with these alterations for all the bridges that were sent to the research group for the limit state of lateral torsional buckling.

The use of a new moment gradient factor, C_b for a non-prismatic member as observed in Section 3.3.1 is recommended. The newly calculated C_b can be used to

Component: Bot CP 1

Load	Load Combo	Limit State	Flexure Type	LL (kip-ft)	Adj. LL (kip-ft)	DC	DW	DW-WS	LL
LegalSpecial	1	STR-I	neg	136.1	---	1.25	1.50	1.50	1.45
LegalSpecial	1	STR-I	neg	-331.2	---	1.25	1.50	1.50	1.45

Legend:
NA - Resistance and live load are of opposite sign so rating factor is not applicable.

fLLz (ksi)	fl (ksi)	Adj. fLLz (ksi)	Phi	fR (ksi)	---- Override ---- Phi	fR (ksi)	RF	Capacity (Ton)
2.38	0.00	---	1.00	-36.00	---	---	NA	NA
-5.79	0.00	---	1.00	-30.86	---	---	3.182	127.27

Figure 3.25 Rating factor–based on effective widths (AASHTO, 2021).

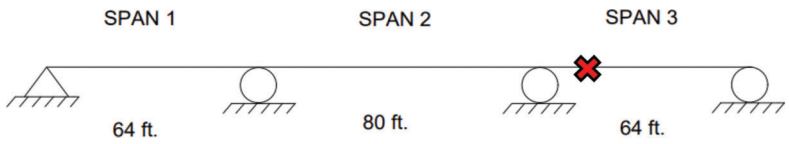

Figure 3.26 Location of the shear spike–I70-076-02376 B.

calculate the new capacity and this new capacity can be used in AASHTOWare BrR by "Capacity Override" as seen in Section 3.3.2.

It is also recommended to model the tapered cover plates differently as shown in Section 3.3.1 instead of using the effective width expression that BrR uses. The approach used by BrR is conservative and produces lesser than anticipated capacity. Instead, the tapered cover plates can be modeled in AASHTOWare BrR as illustrated in the figures in Section 3.3.2.

For the structure P000-47-07089, which had no diaphragms or cross frames providing bracing between the supports, as mentioned in Section 3.3.3, it is recommended to provide a bracing in the second span.

I70-123-02361 JDEB, which passed for all the legal loads except for EV3 lane type legal load for the combination of "truck pair + lane," had a maximum lateral torsional buckling capacity possible i.e., 36 ksi as seen in Section 3.3.3. The recommendation proposed for this bridge was to either strengthen the critical section with splice plates, or steps can be taken to restrict the loads on the bridge. The *INDOT Bridge Inspection Manual* (INDOT, 2020) mentions the emergency vehicle weight limit to be used for EV2 and EV3 trucks. The weight of an EV3 truck is 43 tons and the posting limit specified for 3 axles i.e., EV3 truck is 38 tons (INDOT, 2020). Doing so can ensure that the bridge passes for all the legal loads. Therefore, the corrective actions for lateral torsional buckling are either to add splice plates of suitable length to strengthen the cross section or to restrict the loads for the bridge.

For the structure I70-076-02376 B, abnormal spikes in shear are observed at locations farther from the ends. AASHTOWare BrR works by discretizing the structure into minute elements and each element is defined by two nodes. There was an abnormal rise in the shear force acting from one node to the other as seen. This inconsistency indicates that there is some error with the modelling of the structure in AASHTOWare BrR. An observation was made while finding an explanation for this oddity: the unusual jumps in shears are seen where multiple nodes define the same location on the girder. Future work on the bridge model is needed to correct this problem.

Also, there were three structures, 062-13-07329 A, I465-131-07719 A, and I70-123-02361 DWBL, which rated more than 1.0 as seen before for all the AASHTO and Indiana legal loads. Consequently, there are no recommendations provided for these three structures.

Table 3.10 provides a summary of all the problems and recommendations for all 14 bridges for the controlling limit state of lateral torsional buckling. The No. of the bridges are the same as seen in Table 3.1.

	NODE		SHEAR FORCE (kip)						
	58	0.000	-136.902	0.000	0.000	0.000	583.398	-785.174	-224.468
58	58	0.000	136.902	0.000	0.000	0.000	-583.398	785.174	-224.468
	59	0.000	-142.121	0.000	0.000	0.000	8.166	-382.306	14.745
59	59	0.000	142.121	0.000	0.000	0.000	-8.166	382.306	14.745
	60	0.000	-142.038	0.000	0.000	0.000	16.969	-297.189	14.736
60	60	0.000	142.038	0.000	0.000	0.000	-16.969	297.189	14.736
	61	0.000	-141.956	0.000	0.000	0.000	26.356	-217.064	14.727
61	61	0.000	204.644	0.000	0.000	0.000	-26.356	216.002	14.727
	62	0.000	-164.218	0.000	0.000	0.000	35.982	-4.523	7.502
62	62	0.000	164.218	0.000	0.000	0.000	-35.982	4.523	7.502
	63	0.000	-164.056	0.000	0.000	0.000	210.352	206.546	161.724
63	63	0.000	164.056	0.000	0.000	0.000	-210.352	-206.546	161.724
	64	0.000	-163.812	0.000	0.000	0.000	539.035	537.175	163.219
64	64	0.000	163.812	0.000	0.000	0.000	-539.035	-537.175	163.219
	65	0.000	-163.690	0.000	0.000	0.000	701.551	700.092	163.347
65	65	0.000	163.690	0.000	0.000	0.000	-701.551	-700.092	163.347
	66	0.000	-163.323	0.000	0.000	0.000	1169.470	1168.720	163.097
66	66	0.000	163.323	0.000	0.000	0.000	-1169.470	-1168.720	163.097
	67	0.000	-163.244	0.000	0.000	0.000	1264.279	1263.897	163.194
67	67	0.000	163.244	0.000	0.000	0.000	-1264.279	-1263.897	163.194
	68	0.000	-163.005	0.000	0.000	0.000	1388.245	1388.245	163.005
68	68	0.000	163.005	0.000	0.000	0.000	-1388.245	-1388.245	163.005
	69	0.000	-926.391	0.000	0.000	0.000	1388.222	-1290.915	36.817
69	69	0.000	926.391	0.000	0.000	0.000	-1388.222	1290.915	36.817
	70	0.000	-39.662	0.000	0.000	0.000	1382.121	-1363.222	3.923
70	70	0.000	39.662	0.000	0.000	0.000	-1382.121	1363.222	3.923
	71	0.000	-39.600	0.000	0.000	0.000	1423.767	-1314.933	3.917
71	71	0.000	39.600	0.000	0.000	0.000	-1423.767	1314.933	3.917
	72	0.000	-39.567	0.000	0.000	0.000	1441.754	-1290.285	-13.292
72	72	0.000	39.567	0.000	0.000	0.000	-1441.754	1290.285	-13.292
	73	0.000	-39.561	0.000	0.000	0.000	1443.587	-1285.357	-13.582
73	73	0.000	39.561	0.000	0.000	0.000	-1443.587	1285.357	-13.582
	74	0.000	-39.489	0.000	0.000	0.000	1455.888	-1227.417	-13.388
74	74	0.000	39.489	0.000	0.000	0.000	-1455.888	1227.417	-13.388
	75	0.000	-39.429	0.000	0.000	0.000	1444.251	-1165.635	-30.958
75	75	0.000	39.429	0.000	0.000	0.000	-1444.251	1165.635	-30.958
	76	0.000	-39.377	0.000	0.000	0.000	1390.521	-1091.357	-32.779
76	76	0.000	39.377	0.000	0.000	0.000	-1390.521	1091.357	-32.779
	77	0.000	-39.298	0.000	0.000	0.000	1308.677	-978.758	-33.518
77	77	0.000	39.298	0.000	0.000	0.000	-1308.677	978.758	-33.518
	78	0.000	-39.634	0.000	0.000	0.000	1300.747	-967.985	-34.110

Figure 3.27 Spike in shear values–I70-076-02376 B (AASHTO, 2021).

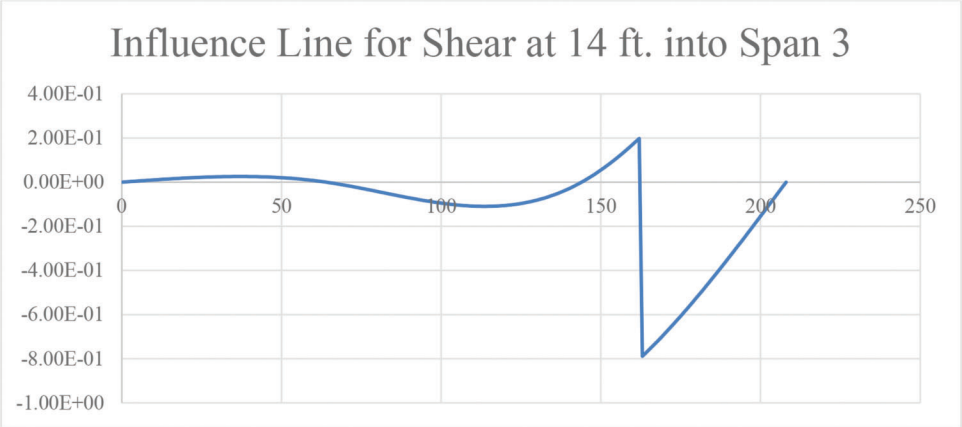

Figure 3.28 Influence lines for shear at 14 ft. into span 3.

TABLE 3.10
Lateral Torsional Buckling–Summary Table

No.	Structure No.	Recommendation
1.	025-09-06941	Stepped beam C_b
2.	I70-008-02344 BWBL	Tapered cover plate
3.	I465-131-07719 A	RF is more than 1.0
4.	I70-079-02420 E	Stepped beam C_b
5.	912-45-06599	Stepped beam C_b
6.	062-13-07329 A	RF is more than 1.0
7.	0I70-076-02376 B	Shear spike
8.	I70-123-02361 JDEB	Load post EV3/Strengthen
9.	I70-123-02361 DWBL	RF is more than 1.0
10.	234-83-07152	Stepped beam C_b
11.	009-30-06644 A	Stepped beam C_b
12.	P000-47-07089	Bracing required
13.	049-64-06679 CNBL	Stepped beam C_b
14.	049-64-06679 CSBL	Stepped beam C_b

4. TIGHT STRINGER SPACINGS

This chapter explores the controlling limit state for tight stringer spacings. Expressions for live load distribution factors are provided in *LRFD Bridge Design Specifications* (AASHTO, 2020). These expressions have limitations on the input variables for their usage. For example, they can be used only for beam center-to-center spacings between 3.5 ft. to 16 ft. For spacing outside of this range, other methods of analysis are recommended to be used. There were 11 bridges reported by INDOT which were adequate for LFR but gave a rating factor for moment of less than 1.0 when rated by LRFR methodology. All these bridges had stringer spacings less than 3.5 ft, therefore they had tight stringer spacings.

4.1 Live Load Distribution Factor

It is necessary to know the effect of the live load acting on each girder of the bridge to calculate the rating factor. The live load distribution factor is a measure used in the *LRFD Bridge Design Specifications* (AASHTO, 2020) to calculate the amount of live load acting on a girder in terms of moment or shear. It is believed to be the controlling factor for the disparity of LFR and LRFR load ratings for tight stringer spacings. Load distribution is calculated differently for the LFR methodology. The following sections explain the procedure used to calculate live load distribution factors for both the methodologies to understand the differences involved.

4.1.1 LFR

The calculation of LL distributions for moment and shear to stringers, longitudinal beams, and floor beams is carried out according to *Standard Specifications for Highway Bridges* (AASHTO, 2002). The flooring between the stringers is assumed to act as a simple span for the lateral distribution of the wheel loads at the ends of the beams or stringers. For other wheel or axle positions, there are prescribed methods as explained below.

For interior stringers and beams, a fraction of a wheel load (both front and rear) is distributed among the stringers. The portion of the load distributed per stringer depends linearly on the spacings between the stringers. The distribution factor varies in value for different kinds of floor types as it can be seen in Figure 4.1. It is a simple linear expression that is to be multiplied with the total live load moment or shear to estimate the effect of the live load on a particular stringer.

For exterior stringers and beams, the calculation of the fraction of the live load bending moment or shear is done by applying the reaction of the wheel load to the stringer or beam by assuming the flooring to act as a simple span between stringer or beams. For dead load effects, the exterior stringer will support the portion of the floor slab that is carried by that particular stringer. All the loads such as curbs, railings and wearing surface if placed after slab curing should be equally distributed among all the stringers or beams.

In general, the load carrying capacity of the exterior stringers should always be greater than the interior stringer. Figure 4.1 shows the expressions used for LL

distribution factors for longitudinal beams for the cases of one lane loaded and two or more lanes loaded.

Here, S denotes the spacing between the beams or stringers (ft.).

The bridges that were evaluated for this study had a reinforced concrete deck on steel I-beam stringers. Therefore, the value of LL distributions for longitudinal stringers should be $\frac{S}{7.0}$ for one traffic lane and $\frac{S}{5.5}$ for two or more traffic lanes.

Kind of Floor	Bridge Designed for One Traffic Lane	Bridge Designed for Two or more Traffic Lanes
Timber:[a]		
Plank[b]	S/4.0	S/3.75
Nail laminated[c]		
4" thick or multiple layer[d] floors over 5" thick	S/4.5	S/4.0
Nail laminated[c]		
6" or more thick	S/5.0 If S exceeds 5′ use footnote f.	S/4.25 If S exceeds 6.5′ use footnote f.
Glued laminated[e]		
Panels on glued laminated stringers		
4" thick	S/4.5	S/4.0
6" or more thick	S/6.0 If S exceeds 6′ use footnote f.	S/5.0 If S exceeds 7.5′ use footnote f.
On steel stringers		
4" thick	S/4.5	S/4.0
6" or more thick	S/5.25 If S exceeds 5.5′ use footnote f.	S/4.5 If S exceeds 7′ use footnote f.
Concrete:		
On steel I-Beam stringers[g] and prestressed concrete girders	S/7.0 If S exceeds 10′ use footnote f.	S/5.5 If S exceeds 14′ use footnote f.
On concrete T-Beams	S/6.5 If S exceeds 6′ use footnote f.	S/6.0 If S exceeds 10′ use footnote f.
On timber stringers	S/6.0 If S exceeds 6′ use footnote f.	S/5.0 If S exceeds 10′ use footnote f.
Concrete box girders[h]	S/8.0 If S exceeds 12′ use footnote f.	S/7.0 If S exceeds 16′ use footnote f.
On steel box girders	See Article 10.39.2.	
On prestressed concrete spread box Beams	See Article 3.28.	
Steel grid:		
(Less than 4" thick)	S/4.5	S/4.0
(4" or more)	S/6.0 If S exceeds 6′ use footnote f.	S/5.0 If S exceeds 10.5′ use footnote f.
Steel bridge Corrugated plank[i]		
(2" min. depth)	S/5.5	S/4.5

Figure 4.1 Live load distribution–LFR (AASHTO, 2002).

4.1.2 LRFR

The distribution factors are calculated according to 4.6.2.2.2 and 4.6.2.2.3 in *LRFD Bridge Design Specifications* (AASHTO, 2020). The expressions may be used for girders, beams, and stringers, except for multiple steel box beams with concrete decks. There are some conditions that must be met for the use of the expressions provided in the AASHTO LRFD Design Manual. These conditions are listed as follows.

- Width of deck is constant.
- The number of beams is not less than four.
- Beams are parallel and have approximately the same stiffness.
- The roadway part of the overhang does not exceed 3 ft.
- Curvature is less than the specified limits.
- Cross section is consistent with the cross sections mentioned in Table 4.6.2.2.1-1 in the *LRFD Bridge Design Specifications* (AASHTO, 2020).

Apart from these general conditions, there are some specific criteria that need to be met for different types of superstructures. This study deals with bridges which a have reinforced concrete slab on steel beams. The deck superstructure of these bridges is Type "a" according to Table 4.6.2.2.1-1 in the *LRFD Bridge Design Specifications* (AASHTO, 2020). The live load distribution factor expressions for interior beams for this type of superstructure are applicable in the girder spacing range of 3.5 ft. and 16 ft. This implies that if the girder spacing does not fall in between 3.5 ft. and 16 ft., the formulae for live load distribution factors cannot be used. In such cases, further analysis is required to calculate the distribution factors.

4.1.2.1 Spacings in 3.5 ≤ S ≤ 16 (ft.). The live load distribution factors for flexural moment in interior beams are calculated according to Table 4.6.2.2.2b-1 in the *AASHTO LRFD Design Manual*. For concrete deck on steel beams, the expressions for distribution factors are given in Figure 4.2.

Here, S is the girder spacing (ft.), L is the span length (ft.), K_g is the longitudinal stiffness parameter, and t_s is

Concrete Deck or Filled Grid, Partially Filled Grid, or Unfilled Grid Deck Composite with Reinforced Concrete Slab on Steel or Concrete Beams; Concrete T-Beams, T- and Double T-Sections	a, e, k and also i, j if sufficiently connected to act as a unit	One Design Lane Loaded: $0.06+\left(\frac{S}{14}\right)^{0.4}\left(\frac{S}{L}\right)^{0.3}\left(\frac{K_g}{12.0Lt_s^3}\right)^{0.1}$ Two or More Design Lanes Loaded: $0.075+\left(\frac{S}{9.5}\right)^{0.6}\left(\frac{S}{L}\right)^{0.2}\left(\frac{K_g}{12.0Lt_s^3}\right)^{0.1}$	$3.5 \le S \le 16.0$ $4.5 \le t_s \le 12.0$ $20 \le L \le 240$ $N_b \ge 4$ $10{,}000 \le K_g \le 7{,}000{,}000$
		use lesser of the values obtained from the equation above with $N_b = 3$ or the lever rule	$N_b = 3$

Figure 4.2 Live load distribution–LRFR (AASHTO, 2020).

the thickness of the slab. The longitudinal stiffness parameter, K_g is taken as:

$$K_g = n\left(I + Ae_g^2\right) \qquad \text{(Equation 4.1)}$$

Where, n is the ratio of moduli of elasticity of the beam material and deck material, I is the moment of inertia of the non-composite beam (in.^{4}), A is the cross section are of non-composite beam (in.^{2}), and e_g is the distance between centers of gravity of the basic beam and deck (in.).

4.1.2.2 Lever rule. The *LRFD Bridge Design Specifications* (AASHTO, 2020) recommend the use of the lever rule for cases where the formulae to calculate distribution factors are not applicable. The lever rule is an approximate method of analysis which assumes the transverse deck cross section to be statically determinate and, hence, uses statics and direct equilibrium to determine the load distribution to a beam of interest.

The bridges provided by INDOT with low LRFR rating factors for the controlling limit state for tight stringer spacings had stringer spacings as shown in Table 4.1.

As can be seen, the stringer spacings for all of the bridges are less than 3.5 ft. and thus they do not lie in the range of applicability as per the *LRFD Bridge Design Specifications* (AASHTO, 2020). Therefore, the use of lever rule is recommended to calculate the distribution factors.

Although AASHTO LRFD suggests the use of lever rule, it has been demonstrated by Yousif and Hindi (2007) that the LRFD methodology overestimates the live load distribution when compared to finite element analysis specifically when lever rule is used. The LL distribution produced by finite element analysis was about 55% less than values obtained by using lever rule. Yousif and Hindi (2007) also suggested that the LRFD methodology gave comparable results to the finite element for bridges with parameters within intermediate ranges and tends to deviate within the extreme ranges of applicability. Since the stringer spacings are less than 3.5 ft. for the concerned bridges, the LRFD methodology does not produce reliable LL distribution factors.

TABLE 4.1
Structures with Tight Stringer Spacings and Low LRFR Ratings

No.	NBI No.	INDOT Str. No.	Spacing (ft.)
1.	300	001-68-03408 B	3.083
2.	7040	026-38-03430 A	3.083
3.	15790	042-11-03101 C	3.375
4.	15830	042-67-03172 B	3.375, 3.229
5.	17540	046-15-01987 A	3.333
6.	24970	075-08-03653 B	3.417, 3.333
7.	26700	135-55-01522 B	3.333
8.	28420	163-83-01393 A	3.333
9.	29150	225-79-04016 G	3.083
10.	30840	256-36-03370 B	3.333
11.	60090	P000-57-07062	3.333

4.2 Work Done in Tennessee–Distribution Factor

4.2.1 Henry's Method–Simplified Approach

A simplified method, known simply as Henry's method, was presented by Huo et al. (2004) for the calculation of distribution factors of live load moment and shear. In this paper it is demonstrated that the moment live-load distribution factors for 24 actual bridges of 6 different bridge types were reasonably calculated using Henry's method when compared with values from both AASHTO and finite-element models. Questions have been raised about the unconservative nature of Henry's method for calculating shear live-load distribution factors, but the moment distribution factors are believed to be accurate. Moreover, for the eleven bridges of concern by INDOT the shear limit state for tight stringers rated greater than 1.0 by LRFR; the moment limit state for tight stringer spacings were the values rating less than 1.0 by LRFR. Consequently, the use of Henry's method discussed herein is for moment live-load distribution factors.

The calculations of the distribution factors showcasing the lever rule and Henry's method for one of the bridges identified by INDOT is presented below.

INDOT Str. No. (Bridge ID): 075-08-03653 B
Stringer spacing=3.333 ft.
Width of roadway=28 ft.
Number of stringer lines=10

1. Dividing the roadway width by 10 ft. to determine the fractional number of traffic lanes.
$$\frac{28}{10} = 2.8$$
2. Calculating MPF by linear interpolation.
For 2 lane bridge, MPF=1 (100%).
For 3 lane bridge, MPF=0.9 (90%).
Therefore, by linear interpolation, for 2.8 lanes,
1 – {(2.8 – 2) * (1 – 0.9)}=0.92
thus, the MPF is 0.92.
3. Reducing the value from step 1 by the multiple presence factor (MPF).
2.8 * 0.92=2.576
4. Dividing the total number of lanes by the number of beam lines and multiplying by $\frac{6}{5.5}$
$$\frac{2.576}{10} * \frac{6}{5.5} = 0.281$$

Therefore, the value of distribution factor using Henry's method is 0.281. (It should be noted that the 10-ft. roadway width in Step 1 is prescribed in the methodology, and that the use of a 12-ft. roadway width will actually result in a lower distribution factor.)

The value computed by lever rule and what BrR uses is 0.6 for one lane and 0.5 for multi-lane. It is evident that this value is significantly higher than the value produced by Henry's method. The screenshot

below shown as Figure 4.3 has been taken from BrR and it shows the distribution factor calculated by lever rule.

There is a steep jump in the values of the LLDF seen if we move from a girder spacing of 3.333 ft. to 3.5 ft. If the girder spacing is 3.5 ft., then according to *LRFD Bridge Design Specifications* (AASHTO, 2020), the following expressions are used.

One Design Lane Loaded:

$$0.06+\left(\frac{S}{14}\right)^{0.4}\left(\frac{S}{L}\right)^{0.3}\left(\frac{K_g}{12Lt_s^3}\right)^{0.1}$$

Two or More Design Lanes Loaded:

$$0.075+\left(\frac{S}{9.5}\right)^{0.6}\left(\frac{S}{L}\right)^{0.2}\left(\frac{K_g}{12Lt_s^3}\right)^{0.1}$$

Using these expressions, the value of LLDF for a girder spacing of 3.5 ft. for the Str No. 075-08-03653 B comes out to be equal to 0.334 for one design lane loaded and 0.381 for two or more design lanes loaded. Therefore, by moving the spacing by about 2 in., there is a jump in the LLDF values. This demonstrates that the lever rule is certainly conservative.

If it assumed, as per Yousif and Hindi (2007), that there is a 55% error by the lever rule in this lower range of stringer spacing, then FEM would give (0.6) * (1 – 0.55) = 0.27. This value is fairly close to the value of 0.281 produced by Henry's method. As the value of the distribution factor calculated by BrR (lever rule) is greater than the value computed by Henry's method, the value of LL effects on the girder are higher. Higher live load effects result in smaller rating factor values, and this can also be seen from the rating factor equation. The denominator part of the rating factor equation signifies the live load effects and as the denominator increases (by lever rule), the rating factor value decreases.

4.3 Recommendations

4.3.1 General

It is seen in the previous sections that the lever rule can overestimate the value of live load distribution. Thus, the use of Henry's method is recommended for the bridges instead of lever rule. The calculation of live load distribution by Henry's method is a simplified process and it can be calculated separately. This can be done using a simple Excel file as shown in Table 4.2.

The next section describes how the distribution factor computed by Henry's method can be used in AASHTOWare BrR.

4.3.2 AASHTOWare BrR

The distribution factor computed using Henry's method can be inputted in BrR as shown in the screenshots below.

1. Distribution factor taken by default–lever rule. Figure 4.4 illustrates the distribution factors for one lane and multi lane that are used by AASHTOWare BrR, computed according to the lever rule. The distribution factor is calculated by lever rule as 0.6 for one-lane and 0.5 for multi-lane according to *LRFD Bridge Design Specifications* (AASHTO, 2020).
2. Rating factor after running the analysis–lever rule. Figure 4.5 shows the value of the rating factor as 0.674, that is calculated by using the LL distributions computed by lever rule.
3. Inputting the new distribution factor–Henry's method. The new LL distribution calculated by using Henry's method can be inputted by manually editing the existing values of 0.6 and 0.5 in Figure 4.4. Figure 4.6 shows the new values of distribution factors that are inserted. No other changes are made, just the previous values are

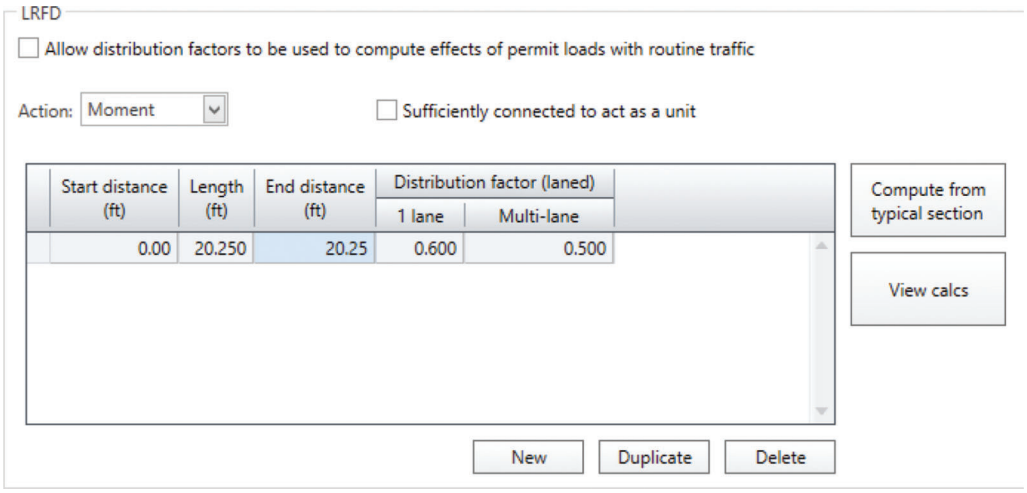

Figure 4.3 Distribution factor (lever rule)–AASHTOWare BrR (AASHTO, 2021).

TABLE 4.2
Henry's Method-Distribution Factor

Structure No.	Roadway Width	No. of Girder Lines	No. of Traffic Lanes	MPF	Reduced Value	Dist. Factor
075-08-03653 B	28	10	2.8	0.92	2.576	0.281018
026-38-03430 A	26	10	2.6	0.94	2.444	0.266618
042-67-03172 B	24	8	2.4	0.96	2.304	0.314182
135-55-01522 B	24	8	2.4	0.96	2.304	0.314182
163-83-01393 A	24	8	2.4	0.96	2.304	0.314182
046-15-01987 A	24	8	2.4	0.96	2.304	0.314182
042-11-03101 C	24	8	2.4	0.96	2.304	0.314182
001-68-03408 B	28	10	2.8	0.92	2.576	0.281018
225-79-04016 G	14.4167	6	1.44167	0.955833	1.378	0.250545
P000-57-07062	14.5	7	1.45	0.955	1.385	0.215805
256-36-03370 B	24	8	2.4	0.96	2.304	0.314182

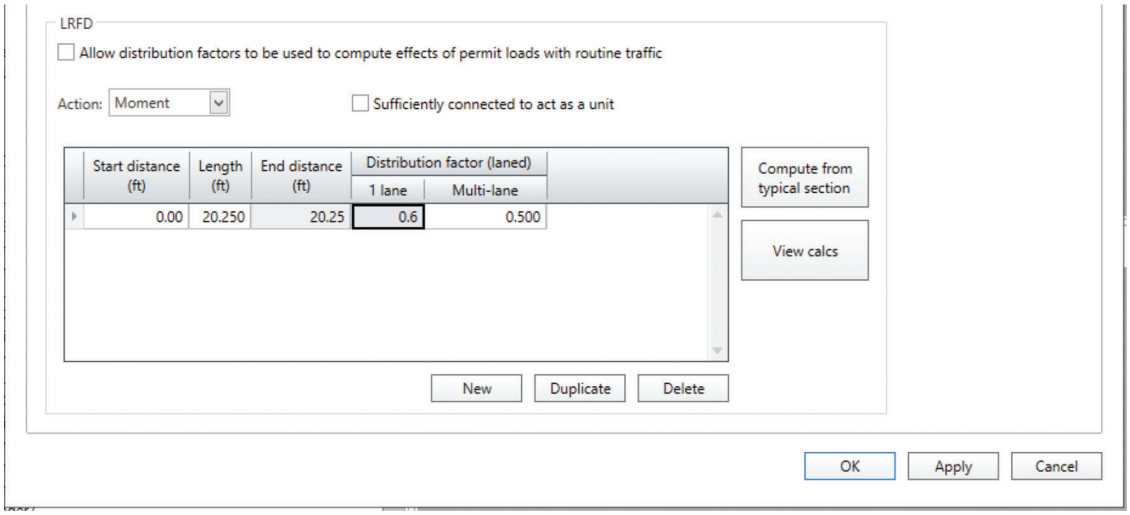

Figure 4.4 Default distribution factor–lever rule (AASHTO, 2021).

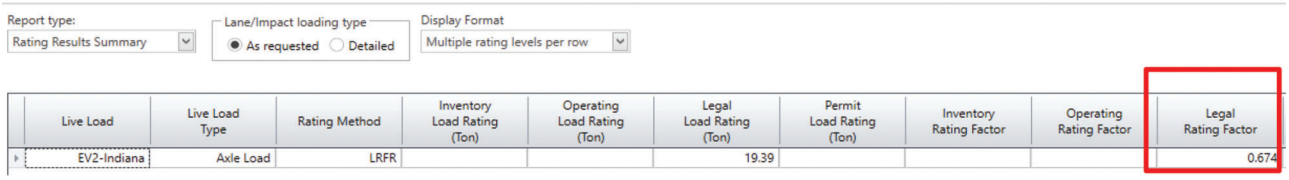

Figure 4.5 Rating factor–lever rule (AASHTO, 2021).

replaced by typing the new value of 0.281 as computed using the Henry's method. By clicking "Apply" and then "OK," the value of LL distribution factor can be updated. Once the value is updated, this value is used in the rating factor calculations performed by BrR.

4. Rating factor after running the analysis–Henry's method. As shown in Figure 4.7, the rating factor calculated now using new the distribution factor is 1.440. The values shown here are for EV2—Indiana for the most critical stringer which is the first interior stringer i.e., Stringer 2. Henry's method produces a rating factor of more than 1.0 for the most critical case, thus it is safe to say that it should work for all the other cases as well. Tables 4.3 and 4.4 show the most critical rating factors for all the bridges calculated by using the LL distribution factors computed by lever rule and Henry's method, respectively.

It is recommended that Henry's method be used for the calculation of live load moment distribution. The new value of distribution factor, as determined by a simple spreadsheet calculation, can be inputted in AASHTOWare BrR software as seen in the example.

There were two structures, P000-57-07062 and 225-79-04016 G, which did not satisfy a rating factor of more than 1.0 even after using the distribution factor by Henry's method. BIAS access was used to generate inspection reports to further investigate these bridges. For P000-57-07062, it was found that this bridge is not

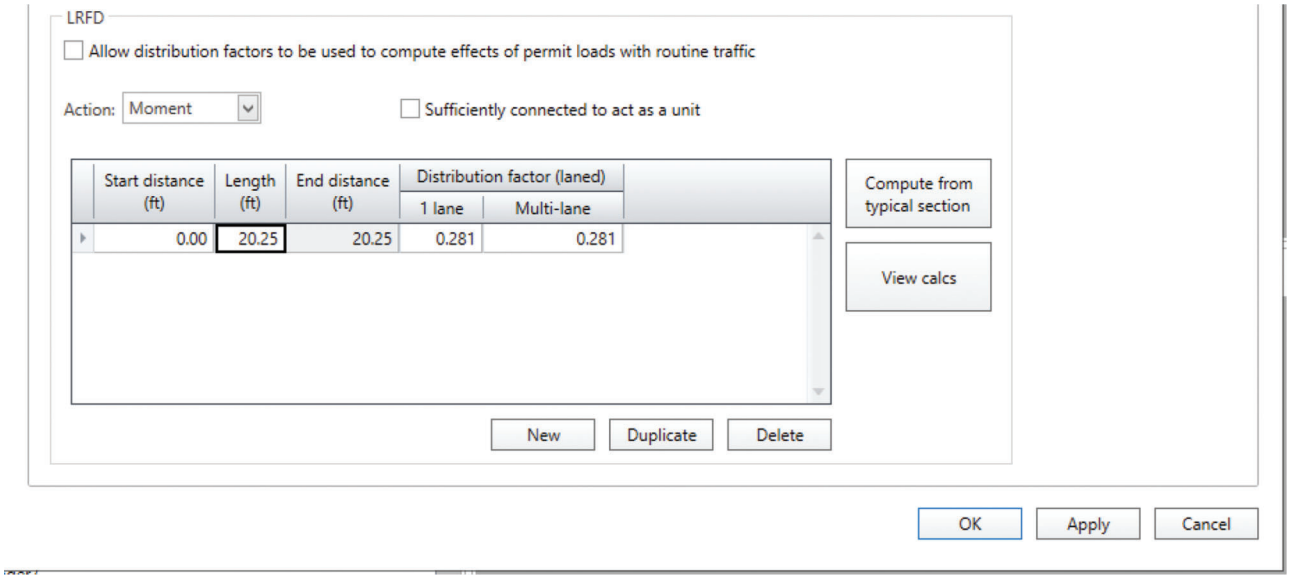

Figure 4.6 Distribution factor–Henry's method (AASHTO, 2021).

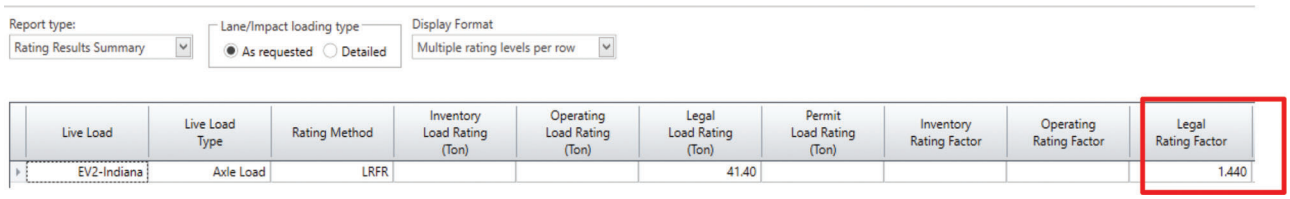

Figure 4.7 New rating factor–Henry's method (AASHTO, 2021).

TABLE 4.3
Rating Factors–Lever Rule

No.	Structure No.	Distribution Factor		Rating Factor
		One Lane	Multilane	
1.	001-68-03408 B	0.6	0.5	0.749
2.	026-38-03430 A	0.6	0.5	0.817
3.	042-11-03101 C	0.6	0.5	0.725
4.	042-67-03172 A	0.6	0.5	0.699
5.	046-15-01987 A	0.6	0.5	0.701
6.	075-08-03653 B	0.6	0.5	0.674
7.	135-55-01522 B	0.6	0.5	0.670
8.	163-83-01393 A	0.6	0.5	0.698
9.	256-36-03370 B	0.6	0.5	0.692

TABLE 4.4
Rating Factors–Henry's Method

No.	Structure No.	Distribution Factor	Rating Factor
1.	001-68-03408 B	0.281	1.600
2.	026-38-03430 A	0.266	1.843
3.	042-11-03101 C	0.314	1.385
4.	042-67-03172 A	0.314	1.335
5.	046-15-01987 A	0.314	1.339
6.	075-08-03653 B	0.281	1.440
7.	135-55-01522 B	0.314	1.280
8.	163-83-01393 A	0.314	1.334
9.	256-36-03370 B	0.314	1.321

adequate even for LFR methodology. The report clearly mentioned that the structure has a critical condition and there is advanced section loss of the primary structural components. It also indicated that the bridge is open to public but now is load posted. The bridge inspection report for 225-79-04016 G suggested that the condition of the deck and the superstructure has advanced deterioration. The condition of the wearing surface is poor while that of the substructure is fair. It is also to be noted that the load rating this structure is inadequate even for the LFR methodology; the structure is currently load posted. Rehabilitation or replacement of structural components is necessary to improve the load rating and remove the load posting.

5. GIRDER END SHEAR AND MOMENT OVER CONTINUOUS PIERS

This chapter discusses the bridges that are rating less than 1.0 by the LRFR methodology for the limit states of shear at girder ends and moment over continuous piers. The ratings for the shear and flexure limit states were examined and the objective was to find repeatable trends for rating factors less than 1. The bridge inventory to examine for this limit state included all

the bridges that were inspected for the limit state of lateral torsional buckling and two additional bridges sent by INDOT. Table 5.1 lists all the bridges that were investigated.

These bridges were run in BrR for both LFR and LRFR and the results were compared. The bridges from No. 1 to 14 are the ones that were investigated for the limit state of lateral torsional buckling and were examined in depth in Chapter 3. It was observed that all of these bridges passed for the limit state of shear. They were found to have an insufficient rating factor for flexure, either at the piers or within the span, but as these bridges were explored in detail in Chapter 3, the same recommendations can be provided here to resolve the discrepancy. Bridge No. 15 and 16 are the two additional bridges that are introduced in this chapter. The discussion regarding these bridges is provided in the following paragraphs.

The structure I65-176-05509 showed unusual results, very similar to I70-076-02376 B, as noted in Section 3.3.3. This structure consists of five spans and the bridge is inadequate for shear at the center of the second span as shown in Figure 5.1 when rated by the LRFR methodology. As observed in Section 3.3.3, there was a spike in shear, this time observed at the center of span 2. This abnormal increase in shear force led the rating factor being extremely low at that location.

Figure 5.2 illustrates the spike in shear. It represents the report generated for EV3 Legal Truck for LRFR analysis in AASHTOWare BrR.

TABLE 5.1
Bridge Inventory–Girder End Shear and Moment Over Continuous Piers

No.	Structure No.
1.	049-64-06679 CNBL
2.	049-64-06679 CSBL
3.	912-45-06599
4.	009-30-06644 A
5.	234-83-07152
6.	025-09-06941
7.	I70-008-02344 BWBL
8.	062-13-07329 A
9.	I465-131-07719 A
10.	I70-123-02361 DWBL
11.	P000-47-07089
12.	I70-079-02420 E
13.	I70-076-02376 B
14.	I70-123-02361 JDEB
15.	B I65-176-05509 BSBL
16.	163-83-05325

Here, nodes 38 and 39 denote the middle of span 2 and there is a sudden jump observed from node 38 (-36.798 kips) to node 39 (-714.815 kips). The value of -714.815 kips is extremely high and, as noted earlier, such a high value at the middle of span is not justified.

A separate analysis was run in SAP2000 similar to the structure I70-076-02376 B noted earlier in Section 3.3.3, to verify the values produced by AASHTOWare BrR.

Again, the method of influence lines was used to calculate the maximum value of shear produced by an EV3 Truck at the center of span 2. The influence line for shear at the center of span 2 is shown in Figure 5.3. The calculated value was -34.39 kips. Thus, the shear of -36.798 kips can be justified, but the sudden spike cannot.

As already noted in Chapter 3, the modelling of the structure in BrR has some errors. Future work on the model is needed to rectify the discretization of the structure into elements, especially at the locations where multiple nodes define a single location.

The structure 163-83-05325 (S. No. 16) was the last bridge to be investigated for this limit state. This bridge was adequate for shear at all the locations. It was found to be inadequate in flexure at an interior pier and the reasons for the deficiency were investigated. It was observed that the lateral torsional buckling capacity of the girder was exceptionally low. When the reasons for the low lateral torsional buckling capacity were investigated, it was noted that the moment gradient factor, C_b was considered as 1.0 since the member was non-prismatic within the unbraced length. The calculation of C_b for stepped beams (Park & Stallings, 2003) can be implemented here to provide a new C_b. It was also observed that the girder consisted of a tapered cover plate which can be modelled using the concept explored in Chapter 3. The girder elevation within the unbraced length is shown in Figure 5.4.

1. It can be seen from the BrR analysis results that there is one inflection point within the unbraced length. Therefore,

$$C_{bst} = \frac{10M_{max}}{4M_{max} + M_A + 7M_B + M_C}$$

M_{max}=1,377.15 kip − ft
M_A=1,062.99 kip − ft
M_B=779.27 kip − ft
M_C=539.41 kip − ft

$$C_{bst} = \frac{10(1{,}377.15)}{4(1{,}377.15) + (1{,}062.99) + 7(779.27) + (539.41)} = 1.096$$

2. The next step is to find C_{st}. The equation for a singly stepped beam is,

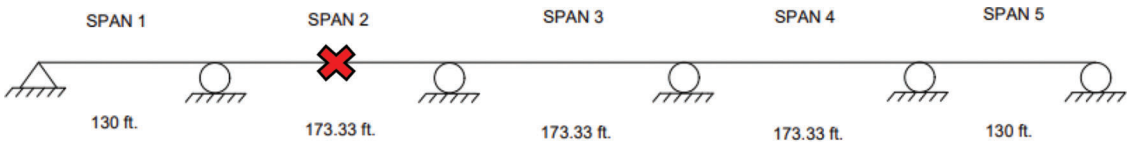

Figure 5.1 Location of the shear spike–I65-176-05509.

Element Actions

Load Case: Load Case 1 - Maximum Effects for EV3 - Indiana - Legal Truck
Load ID: 1

	NODE		SHEAR FORCE (kip)						
36	36	0.000	36.798	0.000	0.000	0.000	-880.891	-418.839	21.259
	37	0.000	-36.798	0.000	0.000	0.000	1019.072	658.022	21.259
37	37	0.000	36.798	0.000	0.000	0.000	-1019.072	-658.022	21.259
	38	0.000	-36.798	0.000	0.000	0.000	1249.378	1056.668	21.259
38	38	0.000	36.798	0.000	0.000	0.000	-1249.378	-1056.668	21.259
	39	0.000	-714.81	0.000	0.000	0.000	1249.366	-2189.839	153.997
39	39	0.000	714.815	0.000	0.000	0.000	-1249.366	2189.839	153.997
	40	0.000	-107.570	0.000	0.000	0.000	861.790	-1083.657	-17.991
40	40	0.000	107.570	0.000	0.000	0.000	-861.790	1083.657	-17.991
	41	0.000	-98.905	0.000	0.000	0.000	744.842	-520.093	-17.991
41	41	0.000	98.905	0.000	0.000	0.000	-744.842	520.093	-17.991
	42	0.000	-92.434	0.000	0.000	0.000	666.883	-167.459	-17.991
42	42	0.000	92.434	0.000	0.000	0.000	-666.883	167.459	-17.991
	43	0.000	-75.270	0.000	0.000	0.000	528.884	528.884	75.270
43	43	0.000	75.270	0.000	0.000	0.000	-528.884	-528.884	75.270
	44	0.000	-71.664	0.000	0.000	0.000	636.971	636.971	71.664
44	44	0.000	71.664	0.000	0.000	0.000	-636.971	-636.971	71.664
	45	0.000	-57.123	0.000	0.000	0.000	953.481	940.947	31.500
45	45	0.000	57.123	0.000	0.000	0.000	-953.481	-940.947	31.500
	46	0.000	-51.489	0.000	0.000	0.000	1028.738	1003.074	25.894
46	46	0.000	51.489	0.000	0.000	0.000	-1028.738	-1003.074	25.894
	47	0.000	-42.604	0.000	0.000	0.000	1101.649	1039.719	33.330
47	47	0.000	42.604	0.000	0.000	0.000	-1101.649	-1039.719	33.330
	48	0.000	-39.885	0.000	0.000	0.000	1118.358	-86.305	29.703
48	48	0.000	39.885	0.000	0.000	0.000	-1118.358	86.305	29.703
	49	0.000	-39.885	0.000	0.000	0.000	1121.481	-26.466	27.198
49	49	0.000	39.885	0.000	0.000	0.000	-1121.481	26.466	27.198
	50	0.000	-39.885	0.000	0.000	0.000	1023.645	345.787	-46.367
50	50	0.000	39.885	0.000	0.000	0.000	-1023.645	-345.787	-46.367
	51	0.000	-39.885	0.000	0.000	0.000	902.770	518.636	-53.498
51	51	0.000	39.885	0.000	0.000	0.000	-902.770	-518.636	-53.498
	52	0.000	-39.885	0.000	0.000	0.000	804.296	777.879	38.401
52	52	0.000	39.885	0.000	0.000	0.000	-804.296	-777.879	38.401
	53	0.000	-39.885	0.000	0.000	0.000	1226.747	1209.970	39.520
53	53	0.000	39.885	0.000	0.000	0.000	-1226.747	-1209.970	39.520
	54	0.000	-39.883	0.000	0.000	0.000	1226.754	1209.977	39.514

Figure 5.2 Spike in shear values–I65-176-05509 (AASHTO, 2021).

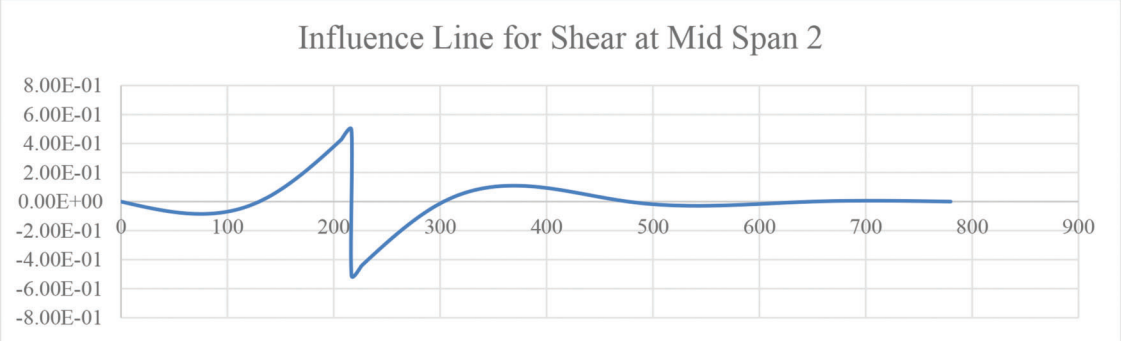

Figure 5.3 Influence lines for shear at center of span 2.

$C_{st} = C_o + 1.5\ \alpha^{1.6}(\beta\gamma^{1.2} - 1)$

$\alpha = \frac{16.5}{24.07} = 0.686,\ \beta = \frac{11.975}{11.95} = 1.002,\ \gamma = \frac{0.94}{0.79} = 1.19$

$C_o = 1$ C_o, as there is one inflection points within the unbraced length.

Therefore,

$C_{st} = 1 + 1.5 * (0.686)^{1.6}(1.002 * (1.19)^{1.2} - 1) = 1.193$

Thus,

$C_b = C_{bst} C_{st} = 1.096 * 1.193 = 1.308$

Thus, the new C_b is calculated to be equal to 1.308.

Apart from modifying the moment gradient factor, the modelling of cover plate is also suggested to be done for this beam. The cover plate of this beam resembles the one as shown in Figure 3.15. The new effective width is calculated by using Equation 3.29,

$$b_{eff} = \left\{\frac{(B1 + B2)}{2} * \frac{L1}{2L1 + L2}\right\} + \left\{B2 * \frac{L2}{2L1 + L2}\right\} + \left\{\frac{(B1 + B2)}{2} * \frac{L1}{2L1 + L2}\right\}$$

where, B1=3 in., B2=11 in., L1=2 ft., and L2=39 ft.

$$b_{eff} = \left\{\frac{(3\text{in} + 11\text{in})}{2} * \frac{2}{2 * 2\text{ft} + 39\text{ft}}\right\} + \left\{11 * \frac{39\text{ft}}{2 * 2\text{ft} + 39\text{ft}}\right\} + \left\{\frac{(3\text{in} + 11\text{in})}{2} * \frac{2\text{ft}}{2 * 2\text{ft} + 39\text{ft}}\right\}$$

This results in an effective width of 10.62 in. Using the new C_b and the effective width of the cover plate, the capacity of the unbraced length can be modified in AASHTOWare BrR as discussed in Section 3.3.2. The rating factors before and after modification are shown in the screenshots below in Figure 5.5 and Figure 5.6. The critical loading for this case was the NRL legal truck which is shown here.

The rating factor drastically increases from 0.170 to 2.269 by using the new C_b and the effective width of the tapered cover plate.

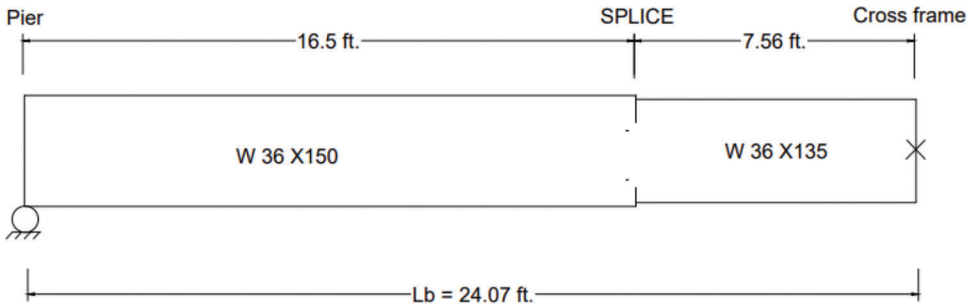

Figure 5.4 Girder elevation–unbraced length.

Component: Bot CP 1

Load	Load Combo	Limit State	Flexure Type	LL (kip-ft)	Adj. LL (kip-ft)	DC	DW	DW-WS	LL	fLLz (ksi)
LegalRoutine	1	STR-I	neg	171.2	---	1.25	1.50	1.50	1.30	2.03
LegalRoutine	1	STR-I	neg	-622.1	---	1.25	1.50	1.50	1.30	-7.39

fl (ksi)	Adj. fLLz (ksi)	Phi	fR (ksi)	---- Override ---- Phi	fR (ksi)	RF	Capacity (Ton)
0.00	---	1.00	-12.91	---	---	NA	NA
0.00	---	1.00	-12.91	---	---	0.107	4.29

Figure 5.5 Rating factor for C_b = 1.0.

Component: Bot CP 1

Load	Load Combo	Limit State	Flexure Type	LL (kip-ft)	Adj. LL (kip-ft)	DC	DW	DW-WS	LL	fLLz (ksi)
LegalRoutine	1	STR-I	neg	171.1	---	1.25	1.50	1.50	1.30	2.09
LegalRoutine	1	STR-I	neg	-621.9	---	1.25	1.50	1.50	1.30	-7.61

fl (ksi)	Adj. fLLz (ksi)	---- Override ---- Phi	fR (ksi)	Phi	fR (ksi)	RF	Capacity (Ton)
0.00	---	1.00	-34.70	1.00	-34.70	NA	NA
0.00	---	1.00	-34.70	1.00	-34.70	2.269	90.74

Figure 5.6 Rating factor for $C_b = 1.308$ and $b_{eff} = 10.62$ in.

6. SUMMARY, CONCLUSIONS, AND FUTURE WORK

6.1 Summary, Conclusions, and INDOT Strategic Goal Impact

The study explores the differences between the Load Factor Rating (LFR) and Load and Resistance Factor Rating (LRFR) which lead to the differences between the rating values produced. INDOT developed a list of bridges designed by LFD that were found to be adequate when load rated using LFR, but inadequate for LRFR. There were bridges in five limit states or geometric conditions of interest, namely: lateral torsional buckling, changes in the cross section along the member length, tight stringer spacings, girder end shear, and moment over continuous piers. To better understand differences in the rating values, both the methodologies were studied in detail and the intrinsic differences owing to the ideology behind the methodologies were noted. These differences produce LRFR rating factors which are generally lower than LFR ratings. The LRFD methodology has some characteristics which tends to make this approach more conservative.

The limit states mentioned above were examined in detail and recommendations were suggested for adapting the AASHTOWare BrR for LRFR when appropriate.

For the limit state of lateral torsional buckling, the calculation of the moment gradient modifier, C_b for non-prismatic sections is assumed to be equal to 1.0 according to the *LRFD Bridge Design Specifications* (AASHTO, 2020), which is a conservative approach. A moment gradient of 1.0 denotes that there is no variation in moment within the unbraced length, which is the worst-case scenario since there is typically a change in the bending moment within the unbraced length if the member is non-prismatic. To rectify this, a new method to calculate C_b is suggested to be used for stepped beams (or non-prismatic sections). This approach ensures that the variation in moment within the unbraced length is considered and the resulting C_b value is higher than 1.0. This newly calculated C_b is used to calculate a new capacity which can be input into AASHTOWare BrR and produce an updated, more accurate rating factor.

Another recommendation that was provided was concerning the modelling of tapered, partial length cover plates in AASHTOWare BrR. AASHTOWare BrR uses a conservative approach to calculate the effective width of tapered cover plates. Instead, a new approach based on the principles of direct proportion of the width within the length in which it occurs is used. The newly modeled cover plate dimensions can then be inputted into AASHTOWare BrR and it results in an increased, more realistic capacity.

For tight stringer spacings, it was observed that the controlling factor for the resulting lower rating factor values by LRFR was the calculation of the live load distribution factors. The formulae in the *LRFD Bridge Design Specifications* (AASHTO, 2020) to calculate LL distributions can be used only if the girder characteristics fall in the range of applicability. If not, then lever rule is used to calculate the LL distributions which is an approach based on statics and is conservative, producing higher than anticipated LL distribution factors (LLDF). The higher live load effects results in lower rating factors. To improve the results produced by lever rule, a technique named Henry's method is suggested to calculate LLDF for stringers with tight spacings (less than 3.5 ft.). The new LLDFs can then be inputted into AASHTOWare BrR and new rating values are generated.

The final limit state that was addressed was girder end shears and moment over continuous piers. For this limit state, all the bridges that were examined for lateral torsional buckling earlier, along with two additional bridges were observed. It was observed that apart from two bridges, all the other bridges were adequate for shear. These two bridges showed an abnormal spike in the shear values within the length of the girder and, therefore, it is believed that the modeling and analysis of the girders in AASHTOWare BrR was flawed. The bridges that were earlier inspected for lateral torsional

buckling for flexure, pass for this limit state as well if the recommendations presented earlier are adopted.

It was observed that the AASHTOWare BrR software generally works well, and other than the possible changes noted in this study, the BrR bridge load rating results should be used. The recommendations suggested in this study can be adopted by INDOT to resolve the problem of inadequacy of bridges by LRFR methodology. These recommendations allow the use of AASHTOWare BrR with some modifications that are more consistent with LFR, and which often result in bridges passing the Load and Resistance Factor Rating (LRFR) as well.

The research in this study impacts the INDOT Strategic goals related to *safety* and *asset sustainability*. Bridge load rating is a technique that is used to assess the adequacy of bridge to carry particular loads. If the bridges in the state system are not able to carry the required AASHTO loads and the State legal loads, then the bridge is considered to be unsafe, and it must be repaired or posted for a limited load capacity. It was shown that the LRFR methodology can be used to safely rate steel bridges in the state inventory when particular modifications are made to account for lateral-torsional buckling of non-prismatic sections and for structures with tight stringer spacings.

6.2 Future Work

Structural testing in a controlled laboratory setting can be performed for bridge sections that are inadequate despite applying the modifications suggested as related to stepped beam C_b, tapered cover plates or Henry's method, for comparisons with AASHTOWare BrR results. The structural laboratory testing of stepped beam sections or members with tapered cover plates will provide useful information on the suitable behavior of those types of members and help to better understand proper modelling assumptions when using AASHTOWare BrR.

Field testing is also an option to evaluate the behavior of the bridges. Strain gages can be used to monitor the effect of live load on the bridge and the results can be checked with BrR results for further evaluation.

Finite Element Analysis (FEA) should be performed to obtain approximate results for stepped beams and tapered cover plates. The results can then be compared with AASHTOWare BrR results. FEA can also be conducted to suggest possible corrections for problematic cases like shear spike that was observed.

REFERENCES

AASHTO. (2002). *Standard specifications for highway bridges* (17th ed.). American Association of State Highway and Transportation Officials.

AASHTO. (2013, August). *AASHTOWare bridge design and rating training: Capacity override at points of interest (BrDR 6.5)* [PDF file]. http://aashtobr.org/wp-content/uploads/2014/09/5-Capacity-Override.pdf

AASHTO. (2018). *The manual for bridge evaluation* (3rd ed.). Association of State Highway and Transportation Officials.

AASHTO. (2020). *LRFD bridge design specifications* (9th ed.). American Association of State Highway and Transportation Officials.

AASHTO. (2021, January). *AASHTOWare bridge rating (BrR) version 7.0.0* [Software]. American Association of State Highway and Transportation Officials.

AISC. (2016, July 7). Specification for structural steel buildings [PDF file]. American Institute of Steel Construction. https://www.aisc.org/globalassets/aisc/publications/standards/a360-16-spec-and-commentary.pdf

Armendariz, R. R., & Bowman, M. D. (2018). *Bridge load rating* (Joint Transportation Research Program Publication No. FHWA/IN/JTRP-2018/07). West Lafayette, IN: Purdue University. https://doi.org/10.5703/1288284316650

CTDOT. (2018, March 29). *CTDOT BrR user guide* [PDF file]. Connecticut Department of Transportation. https://portal.ct.gov/-/media/DOT/documents/dbridgedesign/Load_Rating/BrRUserGuide201810pdf.pdf?la=en

Ghosn, M., & Moses, F. (1998). *Redundancy in highway bridge superstructures* (NCHRP Report 406) [PDF file]. Transportation Research Board. https://onlinepubs.trb.org/onlinepubs/nchrp/nchrp_rpt_406.pdf

Huo, X. S., Wasserman, E. P., & Zhu, P. (2004, July). Simplified method of lateral distribution of live load moment. *Journal of Bridge Engineering*, *9*(4), 382–390. https://ascelibrary.org/doi/abs/10.1061/(ASCE)1084-0702(2004)9:4(382)

INDOT. (2020). *INDOT bridge inspection manual* [PDF file]. Indiana Department of Transportation. https://www.in.gov/dot/div/contracts/standards/bridge/inspector_manual/Bridge_Inspection_Manual.pdf

Joy, E. (2011). *Comparison and study of load and resistance factor rating (LRFR) and load factor rating (LFR) methods* [Master's thesis, University of Cincinnati]. OhioLINK. https://etd.ohiolink.edu/apexprod/rws_olink/r/1501/10?p10_etd_subid=84007&clear=10

Lichtenstein Consulting Engineers, Inc. (2001, May). *Contractor's final report: Manual for condition evaluation and load rating of highway bridges using load and resistance factor philosophy* (NCHRP web document 28) [PDF FILE]. Transportation Research Board. https://onlinepubs.trb.org/onlinepubs/nchrp/nchrp_w28.pdf

Minervino, C., Sivakumar, B., Moses, F., Mertz, D., & Edberg, W. (2004). New AASHTO guide manual for load and resistance factor rating of highway bridges. *Journal of Bridge Engineering*, *9*(1), 43–54. https://ascelibrary.org/doi/abs/10.1061/(ASCE)10840-702(2004)9:1(43)

Moen, C. D., & Fernandez, L. (2009). A comparison of AASHTO bridge load rating methods. *Structures Congress 2009*. https://ascelibrary.org/doi/abs/10.1061/41031(341)52

Moses, F., & Verma, D. (1987, December). *Load capacity evaluation of existing bridges* (NCHRP Report 301). Transportation Research Board.

Murdock, M. (2009, May 21). *Comparative load rating study under LRFR and LFR methodologies for Alabama highway bridges* [Master's thesis, Auburn University]. http://hdl.handle.net/10415/1746

NSC2. (2006, October). *Lateral torsional buckling and slenderness* [PDF file]. http://www.newsteelconstruction.com/wp/wp-content/uploads/TechPaper/NSCOct06_Tech.pdf

Park, J.-S., & Kang, Y. J. (2004). Lateral buckling of stepped beams under linear moment gradient. *Journal of Steel*

Structures, *4*, 71–81. http://www.kssc.or.kr/wonmun/KSSC_3_2004_4_2_71(C).pdf

Park, J. S., & Stallings, J. M. (2003). Lateral-torsional buckling of stepped beams. *Journal of Structural Engineering*, *129*(11), 1457–1465. https://ascelibrary.org/doi/abs/10.1061/(ASCE)0733-9445(2003)129:11(1457)

Park, J. S., & Stallings, M. J. (2005). Lateral-torsional buckling of stepped beams with continuous bracing. *Journal of Bridge Engineering*, *10*(1), 87–95. https://ascelibrary.org/doi/full/10.1061/%28ASCE%291084-0702%282005%2910%3A1%2887%29

Reichenbach, M. C., Liu, Y., Helwig, T. A., & Engelhardt, M. D. (2020). Lateral-torsional buckling of singly symmetric I-girders with stepped flanges. *Journal of Structural Engineering*, *146*(10). https://ascelibrary.org/doi/pdf/10.1061/%28ASCE%29ST.1943-541X.0002780

Sivakumar, B. (2007, August). *The new AASHTO manual for bridge evaluation: A single standard for bridge evaluation* [Conference session]. 4th New York Bridge Conference.

United Consulting. (2017, February 16). *BrR load rating tools and tips* [Powerpoint presentation]. https://www.in.gov/dot/div/contracts/standards/bridges/2017%20Bridge%20Conference/8b_Bridge%20Load%20Rating%20-%20BrR%20Load%20Rating%20Tools%20and%20Tips.pdf

Ward, D. (2019, July 30–31). *AASHTOWare BrR work-arounds* [Powerpoint slides]. https://slideplayer.com/slide/17857814/

Yousif, Z., & Hindi, R. (2007, November). AASHTO-LRFD live load distribution for beam-and-slab bridges: Limitations and applicability. *Journal of Bridge Engineering*, *12*(6), 765–773. https://ascelibrary.org/doi/full/10.1061/%28ASCE%291084-0702%282007%2912%3A6%28765%29

Zheng, L., Huo, S. X., & Hayworth, R. P. (2007). Comparison of load factor rating (LFR) to load and resistance factor rating (LRFR) of prestressed concrete I–beam bridges. *Structures Congress 200*. American Society of Civil Engineers. https://ascelibrary.org/doi/abs/10.1061/40946(248)71

About the Joint Transportation Research Program (JTRP)

On March 11, 1937, the Indiana Legislature passed an act which authorized the Indiana State Highway Commission to cooperate with and assist Purdue University in developing the best methods of improving and maintaining the highways of the state and the respective counties thereof. That collaborative effort was called the Joint Highway Research Project (JHRP). In 1997 the collaborative venture was renamed as the Joint Transportation Research Program (JTRP) to reflect the state and national efforts to integrate the management and operation of various transportation modes.

The first studies of JHRP were concerned with Test Road No. 1—evaluation of the weathering characteristics of stabilized materials. After World War II, the JHRP program grew substantially and was regularly producing technical reports. Over 1,600 technical reports are now available, published as part of the JHRP and subsequently JTRP collaborative venture between Purdue University and what is now the Indiana Department of Transportation.

Free online access to all reports is provided through a unique collaboration between JTRP and Purdue Libraries. These are available at http://docs.lib.purdue.edu/jtrp.

Further information about JTRP and its current research program is available at http://www.purdue.edu/jtrp.

About This Report

An open access version of this publication is available online. See the URL in the citation below.

Khanna, P., & Bowman, M. D. (2021). *Use of LRFR methodology for load rating of INDOT steel bridges* (Joint Transportation Research Program Publication No. FHWA/IN/JTRP-2021/37). West Lafayette, IN: Purdue University. https://doi.org/10.5703/1288284317362